PHYSICAL REVIEW C VOLUME 5, NUMBER 6 JUNE 1972

# Intermediate Structure and the Photodisintegration of $O^{16}$†*

Wayne L. Wang‡
*Department of Nuclear Engineering, Massachusetts Institute of Technology, Cambridge, Massachusetts 02139*

and

C. M. Shakin
*Department of Physics, Case Western Reserve University, Cleveland, Ohio 44106*
(Received 28 October 1971)

A theory of photonuclear reactions is formulated using a projection-operator formalism. We obtain a $T$ matrix describing a direct photoeffect and a resonance reaction. By introducing doorway and secondary-doorway states, we can conveniently study the structure and energy dependence of the $T$ matrix.

The formalism is applied to the analysis of the photonuclear cross sections of $O^{16}$. The $(\gamma,n)$ and $(\gamma,p)$ cross sections are calculated. We consider those channels in which the residual nucleus is left in the ground state ($J^\pi=\frac{1}{2}^-$) or the third excited state ($J^\pi=\frac{3}{2}^-$). In the shell-model formulation, the doorways are taken to be mixtures of 1p-1h states, which are constructed in the Tamm-Dancoff approximation. The secondary doorways are assumed to be 3p-3h states, which are constructed in the interacting-boson approximation of Iachello and Feshbach. By mixing the doorways and the secondary doorways, we obtain a microscopic description of the compound states formed in the reactions. The doorways are shown to be responsible for the gross structure of the giant dipole resonances, while their couplings to the secondary doorways give rise to intermediate structure. A particular model of the 3p-3h states, together with certain simplifications in the description of the reaction, reproduces some of the experimental data (the photodisintegration to the $J^\pi=\frac{1}{2}^-$ ground state) to a surprising degree of accuracy.

The calculation evidently shows the importance of the 3p-3h admixture in the low-lying odd-parity states of $O^{16}$. Our results also give strong support to assigning $E1$ nature to the resonances at 21.0, 22.3, 23.1, 24.2, 25.2, and 25.6 MeV.

## I. INTRODUCTION

Photonuclear disintegration of $O^{16}$ has been a very interesting subject for both experimental and theoretical investigations. The gross features of the cross sections have long been explained as due to excitations of one-particle–one-hole (1p-1h) configurations.[1] These calculations, despite their differences, come to essentially the same conclusions, and suffer from the same shortcomings. In the giant dipole region (20–26 MeV), theories predict two major resonances, at 22.3 and 24.5 MeV, which carry almost all the dipole sum.[2] This is in contrast with the experimental observations; the cross sections show a much more complex structure. Experimentally, there are *at least* five distinct resonances in this region; roughly they occur at 21, 22, 23, 24, and 25 MeV in both $\sigma(\gamma,n)$[3] and $\sigma(\gamma,p)$.[4] For convenience, we shall call such features "intermediate structure" and reserve the term "fine structure" for the structure appearing with even higher resolution.[5] Experimentally, such structure is so well established that the simple 1p-1h calculations may be considered inadequate and we require a more sophisticated theoretical interpretation.

A natural extension of the calculations is, of course, the inclusion of more complicated nuclear excitations in the reaction formalism.[6] Such attempts have already been made, for example, in the work of Gillet, Melkanoff, and Raynal,[7] and Balashov and Kabachnik,[7] who extended the calculation to include 2p-2h configurations. These calculations use a microscopic description, but are somewhat schematic and qualitative. On the other hand, the dynamic collective model has been employed by several authors[8] who included the coupling of the dipole states to the quadrupole surface vibrations of the nucleus. These collective descriptions in their simplest form may not be relevant to the oxygen nucleus.

In the following we propose an alternative microscopic interpretation of the intermediate structure within nuclear shell theory. The problems which we face are twofold: (i) the selection of the nuclear compound states necessary for a sufficiently complete calculation, and (ii) the possible assumptions which we can make for the nuclear reaction mechanisms.

The selection of the relevant compound states in

the energy region of interest is not trivial. To begin with, we make some observations concerning the low-lying states of $O^{16}$. The ground state of $O^{16}$ has been shown by shell-model calculations to contain a large component of deformed 2p-2h and some 4p-4h configurations mixed with the spherical (closed-shell) configuration.[9] It is not unreasonable to expect that the low-lying negative-parity states consist mainly of 1p-1h and 3p-3h configurations. This statement is certainly true if we restrict our model space to the $2s$-$1d$ particle states and the $1p$ hole states in $O^{16}$. It is also clear from the experimental data[3,4,10] that the compound states responsible for the intermediate structure are probably of electric dipole nature ($J^\pi = 1^-, T = 1$). We therefore wish to interpret the compound states in the dipole region as mainly composed of ($J = 1^-, T = 1$) 1p-1h and 3p-3h configurations.[11]

For a simple presentation of the dynamics involved in the reaction processes, we find it useful to use the concept of doorway states.[12] For our purpose, we find it convenient to define primary doorways and secondary doorways. These definitions depend upon the channels in question and the interactions (e.g., electromagnetic or nuclear) coupling the compound states to the channels. Basically, we define *primary doorways* to be states which are strongly coupled to the open channels (nucleon or photon) and the *secondary doorways* are those states which are important in the coupling of the primary doorways to the space of even more complex compound states. In the case of photonuclear reactions, we have the special circumstance that the doorways for photon absorption (1p-1h states) are generally different from the doorways for nucleon emission. In this work we consider only the exit channels for which we may use the *same* doorways for both entrance and exit channels. We will drop the designation "primary" in our discussion and speak only of doorways and secondary doorways. (The latter states have on occasion been called "hallways.") Being strongly mixed with 1p-1h states, some 3p-3h states will be chosen to be the secondary doorways.

The doorways and the secondary doorways are not experimentally observable; only the compound states (mixture of the doorways, secondary doorways, and more complex states) are observed at the resonance energies. The doorway concept, however, is very useful in this reaction theory.

In Sec. II, we present the formalism of photonuclear reactions, formulated in terms of the doorways and the secondary doorways. A projection operator technique[12] is used throughout. We separate our Hilbert space into $P$ (continuum), $d$ (doorway), $q$ (secondary doorway), and $X$ subspaces, and obtain the $T$ matrix with a simple parametrization of the $X$ space. The $T$ matrix contains a direct term and a complicated resonance term. The use of the doorway hypothesis greatly simplifies the structure of the $T$ matrix.

The shell-model wave functions for various states are constructed in Sec. III. The $P$ space is essentially described by continuum, single-particle states of a Woods-Saxon potential. The 1p-1h doorways are constructed in the Tamm-Dancoff approximation (TDA). To construct the complicated 3p-3h states we employ a simplified version of the interacting-boson approximation of Iachello and Feshbach[13] which takes into account the particle-particle and hole-hole interactions, in addition to the particle-hole interaction used to construct the 1p-1h bosons. The coupling of the doorways and secondary doorways is also discussed in detail. Finally, we obtain the compound nuclear states by a diagonalization of the energy matrix in the space of both the doorway and the secondary-doorway states.

We may point out that the doorways and secondary doorways are bound states, in our model description, whose energies are in the continuum of the actual nuclear Hamiltonian. Their unbound (resonance) nature is restored when their couplings to the continuum space are incorporated; such coupling endows each doorway and secondary doorway an energy shift and a width.

The numerical results based on the shell-model formulation are presented in Sec. IV. The gross structure of the ground-state cross section $O^{16}(\gamma, n_0)O^{15}$ is reproduced, in a trial calculation, by including only the doorways. We then calculate the energy-dependent compound shifts and widths of the doorways which, when incorporated into the $T$ matrix, reproduce the intermediate structure. The agreement of this calculation with experiment is excellent. Also we calculate the photoneutron reaction $O^{16}(\gamma, n)O^{15*}$ and photoproton reaction $O^{16}(\gamma, p)N^{15*}$ leading to the third excited state ($J^\pi = \frac{3}{2}^-$) of the residual nucleus.

Concluding remarks are contained in Sec. V. A discussion is also given concerning the experimental support for the parametrization of the $X$ space. This may be of interest for further investigations.

## II. FORMALISM OF PHOTONUCLEAR REACTIONS

The formal theory of photonuclear reactions, in terms of projection operators, has been previously discussed in the simple doorway-state language.[14] Such formalism was applied to reproduce the *gross structure* of the giant dipole reso-

nance of $O^{16}$.[15] We are, however, interested in explaining the intermediate structure existing in this region. For an extension of the doorway-state formalism, we have to include explicitly the coupling of the doorways to more complicated configurations. The concept of such doorway–compound-state coupling has already been employed by Feshbach, Kerman, and Lemmer,[16] in their discussion of the "intermediate structure" associated with the doorways. In the following formulation we also introduce several new features, including the parametrization of the effects of the neglected parts of the nuclear Hilbert space (the $X$ space) and the definition of an intermediate-resolution cross section.

In first-order perturbation theory, the $T$ matrix of interest can be written as

$$T=\langle\Psi^{(-)}|H_\gamma|0\rangle, \tag{1}$$

where $|0\rangle$ is the initial (ground) state of the target nucleus, and $|\Psi^{(-)}\rangle$ is a continuum state. The electromagnetic interaction is $H_\gamma$. We are only concerned with single-nucleon-emission processes to a limited number of open channels; other channels are treated only indirectly.

Let the nuclear Hamiltonian be $H$. We have the Schrödinger equation,

$$(E-H)|\Psi^{(-)}\rangle=0, \tag{2}$$

describing a time-independent state of the nucleus at energy $E$. Following the projection-operator formalism of Feshbach,[12,16] we proceed to classify the states of our nuclear Hilbert space according to their configurations. We make the separation into the one-nucleon continuum space ($P$), the doorway space ($d$), and the complicated space ($Q$), which will be later separated into the secondary-doorway space ($q$) and the $X$ space. (Recall that the secondary doorways are identified as those states of the $Q$ space which are thought to have important coupling to the states of the $d$ space.) The definition of some of these operators and their properties are simply given in Table I. We should particularly note that the $P$ space contains only the open channels which we wish to treat in detail, thus the $X$ space will contain many other open channels.

Following the standard techniques, we obtain the following set of coupled equations[17]:

$$(E-\mathcal{H}_{PP})|P\Psi\rangle=\mathcal{H}_{Pd}|d\Psi\rangle, \tag{3}$$

$$(E-\mathcal{H}_{dd})|d\Psi\rangle=\mathcal{H}_{dP}|P\Psi\rangle, \tag{4}$$

where $\mathcal{H}_{PP}=P\mathcal{H}P$, $\mathcal{H}_{Pd}=P\mathcal{H}d$, and $|P\Psi\rangle=P|\Psi^{(-)}\rangle$, $|d\Psi\rangle=d|\Psi^{(-)}\rangle$, etc. The effective Hamiltonian $\mathcal{H}$ is defined as

$$\mathcal{H}=H+H\frac{Q}{E-H_{QQ}}H. \tag{5}$$

We now have to solve the coupled equations (3) and (4). The formal solution can be obtained by algebraic methods which yield

$$|P\Psi^{(-)}\rangle=|\psi_0^{(-)}\rangle + \mathcal{G}_P^{(-)}\mathcal{H}_{Pd}\frac{1}{E-\mathcal{H}_{dd}-\mathcal{H}_{dP}\mathcal{G}_P^{(-)}\mathcal{H}_{Pd}}\mathcal{H}_{dP}|\psi_0^{(-)}\rangle, \tag{6}$$

where the homogeneous solutions satisfy

$$(E-\mathcal{H}_{PP})|\psi_0^{(-)}\rangle=0. \tag{7}$$

The Green's function $\mathcal{G}_P^{(-)}$ is defined by

$$\mathcal{G}_P^{(-)}=(E-\mathcal{H}_{PP}-i\epsilon)^{-1}, \tag{8}$$

or equivalently,

$$\mathcal{G}_P^{(-)}=\frac{\mathcal{P}}{E-\mathcal{H}_{PP}}+i\pi\delta(E-\mathcal{H}_{PP}), \tag{9}$$

TABLE I. Definition of the projection operators.

| Operator | Subspace | Description of the configuration |
|---|---|---|
| $P$ | Open-channel space (continuum space) | A continuum nucleon in one of the exit channels to be treated in detail. |
| $d$ | Doorway space | Simple excited states strongly coupled to the incident photon and outgoing nucleon channels. (one-particle–one-hole states) |
| $Q$ | Complicated space | All the possible configurations which are not included in either $P$ or $d$ space. |
| Completeness | $P+d+Q=1$ | |
| Orthogonality | $Pd=dP=0$; $PQ=QP=0$; $Qd=dQ=0$ | |

where $\mathcal{P}$ indicates the principal value. To solve for $|d\Psi\rangle$ in a simple way, we compare the following equation, obtained from Eq. (3),

$$|P\Psi\rangle = |\psi_0^{(-)}\rangle + \mathcal{G}_P^{(-)}\mathcal{H}_{Pd}|d\Psi\rangle, \tag{10}$$

with Eq. (6). We immediately get the result

$$|d\Psi\rangle = (E - \mathcal{H}_{dd} - \mathcal{H}_{dP}\mathcal{G}_P^{(-)}\mathcal{H}_{Pd})^{-1}\mathcal{H}_{dP}|\psi_0^{(-)}\rangle. \tag{11}$$

If the total wave function is written in the following form,

$$|\Psi^{(-)}\rangle = \left(1 + \frac{Q}{E - H_{QQ}}H\right)(|P\Psi\rangle + |d\Psi\rangle), \tag{12}$$

the $T$ matrix can be recast as

$$T = (\langle P\Psi| + \langle d\Psi|)\mathcal{H}_\gamma|0\rangle, \tag{13}$$

where we define a modified photon-interaction operator,

$$\mathcal{H}_\gamma = H_\gamma + \frac{Q}{E - H_{QQ}}H_\gamma. \tag{14}$$

By substitutions we obtain the $T$ matrix for photonuclear reactions,

$$T = \langle\psi_0^{(-)}|\mathcal{H}_\gamma|0\rangle + \langle\psi_0^{(-)}|\mathcal{H}_{Pd}(E - \mathcal{H}_{dd} - \mathcal{H}_{dP}\mathcal{G}_P^{(+)}\mathcal{H}_{Pd})^{-1}(\mathcal{H}_\gamma + \mathcal{H}_{dP}\mathcal{G}_P^{(+)}\mathcal{H}_\gamma)|0\rangle. \tag{15}$$

This is a formal expression; the operators involved are complicated.

In Eq. (15) we have formally suppressed the dependence of the $T$ matrix on the $Q$ space; this is convenient, as the $Q$ space will only be treated in an approximate fashion. We now introduce a complete set of eigenstates in the $d$ space, $\{\phi_d\}$, which is defined by

$$(E_d - H_{dd})|\phi_d\rangle = 0. \tag{16}$$

The introduction of the doorway states in Eq. (15) leads to the $T$ matrix

$$T = \langle\psi_0^{(-)}|\mathcal{H}_\gamma|0\rangle + \sum_d \frac{\langle\psi_0^{(-)}|\mathcal{H}_{Pd}|\phi_d\rangle[\langle\phi_d|\mathcal{H}_\gamma + \mathcal{H}_{dP}\mathcal{G}_P^{(+)}\mathcal{H}_\gamma|0\rangle]}{E - E_d - W_d^\downarrow - W_d^\uparrow}, \tag{17}$$

where we have written the expression so as to facilitate the introduction of the $\{\phi_d\}$ as doorways for the photonuclear reaction. In Eq. (17), we have assumed that the doorway-doorway couplings are diagonal, to simplify the inverse operator in Eq. (15). The *continuum* and the *compound mixings* are defined as

$$W_d^\uparrow = \langle\phi_d|\mathcal{H}_{dP}\mathcal{G}_P^{(+)}\mathcal{H}_{Pd}|\phi_d\rangle, \tag{18}$$

and

$$W_d^\downarrow = \left\langle\phi_d\middle|H_{dQ}\frac{1}{E - H_{QQ}}H_{Qd}\middle|\phi_d\right\rangle, \tag{19}$$

respectively.

The continuum mixing is separated into a *continuum shift* $\Delta_d^\downarrow$ and a *continuum width* $\Gamma_d^\downarrow$ such that

$$W_d^\downarrow = \Delta_d^\downarrow - i\,\Gamma_d^\downarrow/2. \tag{20}$$

We have to introduce the $Q$-space wave functions in the calculation of $W_d^\downarrow$. The $Q$ space contains complicated bound states and also the open channels not included in the $P$ space. Formally we can define a complete set of states in the $Q$ space,

$$(E_Q - H_{QQ})|\Psi_Q\rangle = 0. \tag{21}$$

The compound coupling is then

$$W_d^\downarrow = \sum_Q \frac{\langle\phi_d|H_{dQ}|\Psi_Q\rangle\langle\Psi_Q|H_{Qd}|\phi_d\rangle}{E - E_Q}, \tag{22}$$

where the summation also implies integration over the continuous spectrum of $H_{QQ}$.

Most states in the $Q$ space are too complicated for any detailed theoretical consideration. Depending on the nature of the doorways, a limited set of $Q$ states may be chosen as secondary doorways. The secondary doorways are chosen such that their couplings to the doorways are important. They are the "doorways" connecting our primary doorways to the *rest* of the $Q$ space. To introduce the secondary doorways, we may formally extract from the $Q$ space a subspace, which we define as the $q$ space; the rest of the $Q$ space is then the $X$ space ($Q = q + X$). Following the definition of the doorways, Eq. (16), we may define the secondary doorways $\{\phi_q\}$ by

$$(E_q - H_{qq})|\phi_q\rangle = 0. \tag{23}$$

If we assume that $\phi_q$ and $\phi_{q'}$ are not coupled through the $X$ space we may write the compound mixing as (see Appendix A)

$$W_d^\downarrow = \sum_q \frac{\langle\phi_d|H_{dq}|\phi_q\rangle\langle\phi_q|H_{qd}|\phi_d\rangle}{E - E_q - \Delta_q + i\,\Gamma_q/2} + \Delta_X - i\,\frac{\Gamma_X}{2}, \tag{24}$$

where $\Delta_q - i\,\Gamma_q/2$ parametrizes the couplings of

the secondary doorways to the $X$ space. The coupling of the doorways to the $X$ space is parametrized by the quantity, $\Delta_X - i\,\Gamma_X/2$.

Finally we may define the *compound shifts* and *widths* as

$$\Delta_d^{\downarrow} - i\frac{\Gamma_d^{\downarrow}}{2} = \sum_q \frac{\langle \phi_d | H_{dq} | \phi_q \rangle \langle \phi_q | H_{qd} | \phi_d \rangle}{E - E_q - \Delta_q + i\,\Gamma_q/2} . \tag{25}$$

The matrix now assumes the following form,

$$T = \langle \psi_0^{(-)} | \mathcal{H}_\gamma | 0 \rangle + \sum_d \frac{\langle \psi_0^{(-)} | \mathcal{H}_{Pd} | \phi_d \rangle [\langle \phi_d | \mathcal{H}_\gamma + \mathcal{H}_{dP} \mathcal{G}_P^{(+)} \mathcal{H}_\gamma | 0 \rangle]}{E - E_d - \Delta_d - \Delta_X + i(\Gamma_d + \Gamma_X)/2} , \tag{26}$$

where we have introduced the shift and width parameters,

$$\Delta_d \equiv \Delta_d^{\uparrow} + \Delta_d^{\downarrow} , \tag{27}$$

$$\Gamma_d \equiv \Gamma_d^{\uparrow} + \Gamma_d^{\downarrow} . \tag{28}$$

Equation (26) gives us the $T$ matrix in terms of the continuum states, the doorways, and the secondary doorways as well as the parameters $\Delta_q$, $\Gamma_q$, $\Delta_X$, and $\Gamma_X$. Although we have made use of the usual doorway terminology, the doorway structure in Eq. (26) is only apparent. The operators in the expression involve complete (and very complicated) information about the entire reaction process. Seeking a simplified version of the $T$ matrix, we would like to introduce a hypothesis for the interaction mechanisms.

We assume that the $Q$ space (therefore the secondary doorways) can not be formed directly by the photon interaction with the target and that the $Q$ space is not directly connected to the $P$ space by nuclear forces. Specifically, we make the simplifying assumptions,

$$\langle \Psi_Q | H_\gamma | 0 \rangle = 0 , \tag{29}$$

and

$$\langle \Psi_Q | H_{QP} | \psi_0 \rangle = 0 ; \tag{30}$$

the latter assumption is reasonable for the $O^{16}$ case where we include in the $P$ space only channels in which the residual nucleus, $O^{15}$ or $N^{15}$, is assumed to be in a single-hole state ($p_{1/2}^{-1}$ or $p_{3/2}^{-1}$). Under such a hypothesis, the states $\{\phi_d\}$ act as the doorways for *both* the incident photon and the open nucleon channels. Furthermore we assume that

$$\langle \phi_d | H_\gamma | 0 \rangle \gg \langle \phi_d | H_{dP} \mathcal{G}_P^{(-)} H_\gamma | 0 \rangle . \tag{31}$$

Equation (31) should be well satisfied in the case where there is no single-particle resonance in the $P$ space. Under the assumption of Eq. (31), the doorways are formed *directly* by the photon interaction with the target ground state.

Finally we arrive at the simplest form of the $T$ matrix, which we shall employ in the calculation of the photonuclear cross sections,

$$T = \langle \psi_0^{(-)} | H_\gamma | 0 \rangle + \sum_d \frac{\langle \psi_0^{(-)} | H_{Pd} | \phi_d \rangle \langle \phi_d | H_\gamma | 0 \rangle}{E - E_d - \Delta_d - \Delta_X + i(\Gamma_d + \Gamma_X)/2} . \tag{32}$$

Equation (32) is the central result of this section. Assuming weak doorway-doorway coupling through the continuum and the $q$ space, the sum in Eq. (32) has been reduced to a single sum over *isolated* doorways.

The $T$ matrix we obtain contains a direct term and a resonance term. The direct interaction is generally a smooth function of energy if there are no single-particle resonances. The resonance term may have complicated energy dependence. If the shift $\Delta_d$ and the width $\Gamma_d$ are smooth functions of energy, we see that the resonances, for isolated doorways, would occur near $E_d + \Delta_d + \Delta_X$ and have widths $\Gamma_d + \Gamma_X$. This is the case for the intermediate structure generally discussed. For the energy averaging we have in mind, the situation is different. The $\Delta_d$ and $\Gamma_d$ in Eq. (32) have strong energy dependence due to the compound mixing, $W_d^{\downarrow}(E)$. This feature will give rise to additional resonances and can completely change the resonance structure. The resonance pattern becomes dependent, for known $E_d$'s and $E_q$'s, upon a complete evaluation of the coupling strengths between $|\phi_d\rangle$ and $|\phi_q\rangle$. That is, the matrix elements defining $W_d^{\downarrow}$ must be known.

In our application to the photonuclear giant resonance, we assume that the $|\phi_d\rangle$ are responsible for the gross structure of the giant-resonance cross section. The intermediate structure revealed by better resolution is then interpreted as due to the coupling of the doorways to nearby, more complicated, excitations $|\phi_q\rangle$.

The simplification we have achieved with the doorway hypothesis [and Eq. (31)] should not be overlooked. We have eliminated all the complicated energy dependence due to the propagator $(E - H_{qq})^{-1}$ everywhere except in the term $W_d^{\downarrow}(E)$.

At this point it is useful to review the assumptions that have gone into the derivation of Eq. (32) from the exact formal expression, Eq. (15). The introduction of doorways to describe the photoabsorption process is expected to be an excellent approximation in the resonance region. If the $O^{16}$ ground state is taken to be a doubly closed shell, the appropriate doorways are linear combinations of particle-hole states. (If ground-state correlations are included, it is necessary to consider excitation of particle-hole modes with respect to the

correlated ground state. However, for simplicity we neglect ground-state correlation effects; these effects deserve further study.)

Unlike the case of nucleon elastic scattering, the discussion of photodisintegration from a "doorway" point of view requires the introduction of two types of doorways, doorways for the photoabsorption and doorways for nucleon emission. For the example we have chosen, it is natural to choose the *same* doorways for both these processes. This choice is based on the assumed structure of the final states reached in the reaction, the single-hole states in $O^{15}$ or $N^{15}$. If the states responsible for the intermediate structure (the secondary doorways) are indeed 3p-3h states, simple considerations show that these states are not coupled to the final channels (one continuum particle and one hole), if, as usual, the Hamiltonian contains only two-body forces.

The assumption of the same doorways for both the entrance and exit channel, in addition to simplifying the calculation, has the following important consequence. Inspection of Eq. (32), for example, shows that the angular distribution is governed by the weakly energy-dependent direct process and the resonant doorway-state term. The *magnitude* of the resonant term is modified by the relatively rapid energy dependence of $W_d^{\downarrow}$, particularly that of $\Delta_d^{\downarrow}$ and $\Gamma_d^{\downarrow}$. (In addition, in the doorway model, there is further weak energy dependence of the resonant term due to the energy dependence of the nucleon escape amplitudes of the doorway.)

If we could limit ourselves to $E1$ absorption, then we could conclude that where the resonant part of the $T$ matrix dominates the direct part, that is away from the minima of the resonant part, the shape of the angular distribution should be basically energy-independent. In general, at the minima of the resonant term one may have a somewhat different angular distribution as compared to that at the peaks, since in the former case one has relatively more significant contributions from the direct term. (The direct term will have a somewhat different angular distribution than the resonant term.) This interplay between the direct and resonant amplitudes can also be considered if one tries to explain intermediate structure in the polarization of the nucleons emitted in the photoreaction [see Cole, Firk, and Phillips in Ref. 33].

The experimental studies of Jury, Hewitt, and McNeil[3] and Baglin and Thompson,[4] however, indicate important effects in the angular distribution due to interference of various multipolarities. Further information is needed concerning the $M1$ and $E2$ amplitudes in the resonance region before we can draw any definite conclusions concerning the validity of our doorway hypothesis for the calculation of the $E1$ amplitudes. It is possible that the addition of the *direct* $E2$ amplitude to the $E1$ amplitudes calculated here, might be sufficient to explain most of the characteristics of the observed angular distributions. Further theoretical study of the $E2$ and $M1$ amplitudes in the resonance region are needed before one attempts to fit all the details of the angular distribution in that region.

The foregoing comments concerning the interplay of the direct and resonant amplitudes are made for a single $E1$ doorway. For the photodisintegration of $O^{16}$ there are two important doorways. If it turns out that these doorways have somewhat different ratios of the amplitudes for $s$- and $d$-wave emission, the foregoing comments would then apply to the intermediate structure in the vicinity of each doorway.

If we now consider other final channels, the assumption that we have the *same* doorways for the entrance and exit channels is no longer valid. As an example, we might consider final channels that consist of a continuum particle plus 1p-2h states. For such channels the 1p-1h states (the electromagnetic doorways) *and* the 3p-3h states could be doorways for nucleon emission. In this case, the assumption expressed by Eq. (30) does not hold for the 3p-3h states. If the states $|\phi_d\rangle$ are still taken to be the 1p-1h electromagnetic doorways, the coupling to the final channels is governed by the effective interaction of Eq. (5) rather than by $H_{Pd}$ as in Eq. (32). Thus $\Gamma_d^{\downarrow}$ and $\Delta_d^{\downarrow}$ will take on a more rapid energy dependence. Also, the comments made above concerning the single-doorway dominance of the angular distribution will no longer be valid and the various intermediate-structure peaks *could* have different angular distributions, depending in detail on their 1p-1h and 3p-3h structure. In this more complicated situation it may be simpler to introduce mixtures of 1p-1h and 3p-3h states as doorways rather than the 1p-1h doorways discussed in the foregoing.

With these comments in mind we return to the discussion of the $T$ matrix of Eq. (32). Related to this $T$ matrix we shall define an *intermediate-resolution* cross section $\sigma_I(E)$. We wish to treat the quantities $\Delta_x$, $\Gamma_x$, $\Delta_q$, and $\Gamma_q$ as parameters in the $T$ matrix. As shown in Appendix A, the reduction to the $T$ matrix form of Eq. (32) with *weakly energy-dependent parameters* ($\Delta_x$, $\Gamma_x$, $\Delta_q$, $\Gamma_q$) is only possible if one considers that some energy averaging over the fine structure has been made. Some fine structure would be due to the *discrete* complicated states of the $X$ space (see Appendix A) and would be observed in experiments of greater resolution than are presently available (see, how-

ever, Ref. 5). Let us assume that we carry out the averaging over the fine structure with an energy resolution $\delta E$. We assume that the value of $\delta E$ is chosen as small as possible, but not so small as to leave any significant peaks in the cross section that cannot be explained at the level of complication contained in our $q$-space description. We will term the resulting energy-averaged $T$ matrix of Eq. (32) the *intermediate-resolution* $T$ matrix. (Examples of a gross-resolution $T$ matrix can be found in the 1p-1h calculation with a complex optical potential.) From this $T$ matrix we may define an intermediate-resolution cross section. At this stage we assume that the fluctuation terms are negligible.

Now we should point out that the energy resolution of the experiments we are discussing will probably correspond to a resolution $\Delta E$ which is greater than $\delta E$. We can make contact with experiment by explicitly averaging the intermediate-resolution *cross section* with an experimental resolution function. In our application we choose a Lorentzian resolution function,

$$\rho(E, E') = \left(\frac{\Delta E}{2\pi}\right) \frac{1}{(E-E')^2 + (\Delta E)^2/4}, \tag{33}$$

and the averaged cross section $\sigma(E)$ is given by

$$\sigma(E) = \int \sigma_I(E')\rho(E, E')dE', \tag{34}$$

where $\sigma_I(E)$ is the intermediate-resolution cross section. The definition of $\sigma_I(E)$ and its relation to the parameters are discussed in detail in Appendix A.

We note that the parameters in the $T$ matrix should account for all the neglected nuclear effects (energy averaging and neglected states) on the cross section (see Appendix A). It is therefore important to find a criterion which will determine these parameters. Formally we impose the condition that the parameters should be so chosen as to reproduce the experimental value of the energy-integrated cross section.

In conclusion, we have developed a projection-operator formalism in which intermediate structure in photonuclear cross sections can be discussed in terms of doorways and secondary doorways. We shall begin to utilize a specific nuclear model – the nuclear shell model – to construct the wave functions for each space.

## III. SHELL-MODEL FORMULATION

The nuclear shell model has been used in the analysis of the giant dipole resonance of $O^{16}$. Most of the calculations are, however, restricted to 1p-1h configurations. As these calculations show, the gross structure can be interpreted as due to these excitations. We shall take the doorway configurations to be of this type. We believe that the intermediate structure is due to the mixing of 3p-3h states (taken to be the secondary doorways) with the doorways. Generally 3p-3h states have energies much higher than the dipole states and are thus believed to be unimportant in the splitting of the giant resonance. However we will see that it is possible to find many 3p-3h states in the giant-resonance region. We will use the interacting-boson approximation (IBA) of Iachello and Feshbach, which we shall describe briefly below, to construct our secondary doorways. In this section we will review some aspects of doorway calculations and then indicate how the IBA may be used for our problem. We also discuss the coupling between the doorways and the secondary doorways in detail.

### A. Continuum Space (Ref. 18)

The operator $H_{pp}$ governs the motion of a nucleon in an open channel. The eigenstates of $H_{pp}$ describe a continuum nucleon moving in a field created by the residual nucleus. We make a preliminary definition of a channel vector by

$$|r, c) = \sum_{m, M_I} C^{jIJ}_{mM_IM} a^\dagger_{(l\frac{1}{2})jm}(r)|\lambda I M_I\rangle, \tag{35}$$

where we have characterized the residual nucleus by $|\lambda I M_I\rangle$. Here $\lambda$ and $I$ are the state label and the total angular momentum (with projection $M_I$) of the residual nucleus. The operator $a^\dagger$ creates a spin-$\frac{1}{2}$ particle with orbital angular momentum $l$, total angular momentum $j$, at distance $r$. The total angular momentum $j$ (with projection $m$) is coupled to $I$ to form the channel spin $J$ (with projection $M$). $C^{jIJ}_{mM_IM}$ is a Clebsch-Gordan coefficient. We note that the channel vector $|r, c)$ is not orthogonal to the bound states of the $A$-particle system, since $a^\dagger$ may create a particle in a bound orbital. Therefore $|r, c)$ cannot be used to define our projection operator $P$ for the continuum space. We have to introduce *the* channel vectors $|r, c\rangle$, which are related to $|r, c)$ by

$$|r, c\rangle = (1 - \sum_b |b\rangle\langle b|)|r, c), \tag{36}$$

where $|b\rangle$ denotes the single-particle bound orbitals, occupied and unoccupied, with the same $(l, j)$ quantum numbers as those of the continuum nucleon. In terms of the channel vectors $|r, c\rangle$, the projection operator may be written as

$$P = \sum_c \int |r, c\rangle r^2 dr \langle r, c|, \tag{37}$$

and satisfies the condition $P^2=P$. The $P$ space thus defined is orthogonal to the doorway and the secondary-doorway spaces. An eigenstate of $H_{PP}$ can then be represented in terms of the channel vectors. In case of the absence of channel-channel coupling by $H_{PP}$, we may write the continuum wave function in channel $c$ as

$$P|\Psi_0^{(-)}\rangle=\sum_c \int_0^\infty \frac{v_{c,E}^{(-)}(r)}{r}|r,c\rangle r^2\,dr\,, \tag{38}$$

where the amplitude $v_{c,E}^{(-)}(r)$ is the solution of a single-particle Schrödinger equation,

$$[E-h_c(r)]\frac{v_{c,E}^{(-)}(r)}{r}=0\,. \tag{39}$$

The effective Hamiltonian $h_c(r)$ is a local approximation, diagonal in the channel labels, to the nonlocal operator,

$$h_{cc'}(r,r')=\langle r,c|H_{PP}|r',c'\rangle\,. \tag{40}$$

A reasonable guess for $h_c(r)$ is obtained by identifying this operator with a real optical-model Hamiltonian. Equation (39) becomes

$$\left[\frac{d^2}{dr^2}-k^2-\frac{l(l+1)}{r^2}+U_{lj}(r)\right]v_{lj,E}(r)=0\,, \tag{41}$$

where $U_{lj}(r)$ includes the nuclear and the Coulomb potentials. In Eq. (41) we have restored the $lj$ label for the scattering nucleon. We define $v_{lj,E}^{(-)}=e^{-i\delta_{lj}(E)}v_{lj,E}(r)$, where $\delta_{lj}(E)$ is the phase shift due to the potential $U_{lj}(r)$. Being normalized on energy, the single-particle wave function has the following asymptotic expression:

$$v_{lj,E}(r)\xrightarrow[r\to\infty]{}\left(\frac{k}{\pi E}\right)^{1/2}\sin\left(kr-\frac{\pi l}{2}+\delta_{lj}\right). \tag{42}$$

The main approximation we have made here is the introduction of an average potential, which is local and does not couple different channels. The neglect of channel-channel coupling is reasonable if there is no single-particle resonance in the $P$ space. In case such resonance exists, we have to redefine our $P$ space according to the scheme we have proposed previously.[19] The resulting $P$ space will then contain no resonance.

We next write the $P$-space Green's function in the channel representation,[18,20]

$$G^{(+)}(E)=\sum_c\int\int dr\,r^2|r,c\rangle\frac{g_{c,E}^{(+)}(r,r')}{rr'}\langle r',c|r'^2dr'\,, \tag{43}$$

where the single-particle Green's function $g_{c,E}^{(+)}(r,r')$ is defined as

$$\frac{g_{c,E}^{(+)}(r,r')}{rr'}=\left\langle r,c\left|\frac{1}{E-H_{PP}+i\epsilon}\right|r',c\right\rangle. \tag{44}$$

In terms of regular and irregular solutions of Eq. (41), $v_{c,E}(r)$ and $w_{c,E}(r)$, respectively, the Green's function is

$$\frac{g_{c,E}^{(+)}(r,r')}{rr'}=-\pi\frac{v_{c,E}(r_<)}{rr'}[w_{c,E}(r_>)+iv_{c,E}(r_>)] -\sum_b\frac{\langle r,c|b\rangle\langle b|r',c\rangle}{E-E_b}\,, \tag{45}$$

where $r_<$ and $r_>$ indicate the greater and the lesser of the set $(r,r')$. The last term in Eq. (45) serves to subtract all the bound-state terms in the Green's function and makes its appearance because of the use of the channel vectors $|r,c\rangle$ rather than $|r,c)$ in the definition of $P$ and in Eqs. (37) and (44). The Green's function is to be modified according to Ref. 19, if any single-particle resonance exists in the $P$ space.

### B. Doorway Space

We have defined the doorways for our problem as states of 1p-1h type. These states are excited from the ground state by the electromagnetic interaction and are also strongly coupled to the $P$ space. These 1p-1h doorway configurations are mixed through the residual p-h interactions. The p-h interaction may be simply taken into account in the usual TDA.

First we write the doorway Hamiltonian $H_{dd}$,

$$H_{dd}=d(H_0+V)d\,, \tag{46}$$

where $H_0$ is the sum of the kinetic and potential energies of the independent particles. $V$ is the residual interaction. In Eq. (46) we see that the projected Hamiltonian $H_{dd}$ is identical to the Hamiltonian $H$, as long as we restrict the configurations to be in the $d$ space. We may define a particle-hole state with good $JT$ values as

$$|(j_1j_2^{-1})JMTT_z\rangle=\sum_{\substack{m_1,m_2\\ m_{t_1},m_{t_2}}}C^{j_1j_2J}_{m_1m_2M}C^{\frac12\frac12T}_{m_{t_1}m_{t_2}T_z} \times(-)^{j_2-m_2+\frac12-m_{t_2}} \times a^\dagger_{j_1m_1\frac12m_{t_1}}a_{j_2-m_2\frac12-m_{t_2}}|0\rangle, \tag{47}$$

where $M$ and $T_z$ are the projections of $J$ and $T$, respectively. We shall introduce the convention that a symbol $j$ represents all the single-particle quantum numbers if used *inside* a state vector and if used as an index without accompanying $m$ or $l$ values. Otherwise $j$ represents only the total angular momentum of a single particle. We shall also neglect the projections $(M,T_z)$ in our shorthand notation for Eq. (47): $|(j_1j_2^{-1})JT\rangle$.

For a simple calculation of the particle-hole interaction, we choose the zero-range spin-dependent interaction[20]

$$V_{ij} = -V_0(\pi_t + p\pi_s)\delta(\vec{r}_i - \vec{r}_j), \tag{48}$$

where $V_0$ is the strength of the interaction, related to the oscillator parameter $b$ by

$$V_0 = 8.5\ \text{MeV} \times 4\pi b^3, \tag{49}$$

$p$ is the singlet-to-triplet ratio, and $\pi_s$ and $\pi_t$ are the singlet and triplet spin projection operators. We write the particle-hole matrix element as

$$\langle j_p j_h^{-1} JT | V | j_p' j_h'^{-1} JT \rangle = M(j_p j_h j_p' j_h') F_0, \tag{50}$$

where the coefficient $M(j_p j_h j_p' j_h')$ depends on the geometric factors:

$$M(j_p j_h j_p' j_h') = \frac{(-)^{j_h + j_h' + 1}}{4}[1 + (-)^{l_p + l_h + l_p' + l_h'}]([j_p][j_h][j_p'][j_h'])^{1/2}$$
$$\times\left[\begin{pmatrix} j_p & j_h & J \\ \frac{1}{2} & -\frac{1}{2} & 0 \end{pmatrix}\begin{pmatrix} j_p' & j_h' & J \\ \frac{1}{2} & -\frac{1}{2} & 0 \end{pmatrix}\left\{(1 - 2\delta_{T0}) + \frac{(-)^{l_1 + l_2 + J}}{2}[1 - p - 2\delta_{T0}(1+p)]\right\}\right.$$
$$\left. + \frac{(-)^{l_h + l_h' + j_h + j_h'}}{2}[(1+p) - 2\delta_{T0}(1-p)]\begin{pmatrix} j_p & j_h & J \\ \frac{1}{2} & \frac{1}{2} & -1 \end{pmatrix}\begin{pmatrix} j_p' & j_h' & J \\ \frac{1}{2} & \frac{1}{2} & -1 \end{pmatrix}\right]. \tag{51}$$

The large round brackets denote the Wigner 3-$j$ symbols,[21] $[j] \equiv 2j+1$, and $F_0$ is the radial integral of single-particle wave functions:

$$F_0 = \frac{V_0}{4\pi}\int v_{l_p j_p}(r) v_{l_p' j_p'}(r) v_{l_h j_h}(r) v_{l_h' j_h'}(r) r^{-2} dr. \tag{52}$$

We next turn to the excitation of the particle-hole states by photon interaction (see, for example, the text of Eisenberg and Greiner[22]). In the long-wavelength limit, we may write the photon-nucleus interaction, $H_\gamma$, as the dipole operator,

$$D_\gamma(\mu) = (\tfrac{4}{3}\pi)^{1/2}(ik_\gamma)\sum_{i=1}^{A}\frac{e}{2}\tau_z^i r_i Y_{1\mu}(\hat{r}_i), \tag{53}$$

multiplied by a photon normalization factor $(2\pi\hbar/\omega L^3)^{1/2}$ for a volume $L^3$. Here $k_\gamma$ is the wave number of the photon with energy $\hbar\omega$. Also, $\tau_z$ is the isospin operator with eigenvalue +1 for neutrons and −1 for protons. The matrix element of interest is given as[23,24]

$$\langle j_p j_h^{-1} JT | H_\gamma(\mu) | 0 \rangle = \left(\frac{2\pi\hbar}{\omega L^3}\right)^{1/2}(ik_\gamma) N_{ph} I_0 \delta_{J1}\delta_{M\mu}, \tag{54}$$

where the geometric factor $N_{ph}$ is

$$N_{ph} = \left(\frac{4\pi}{3}\frac{e^2}{8\pi}\right)^{1/2}(-)^{j_2 - 1/2}([l_p][l_h][j_p][j_h])^{1/2}$$
$$\times\begin{pmatrix} l_1 & 1 & l_2 \\ 0 & 0 & 0 \end{pmatrix}\begin{Bmatrix} l_1 & l_2 & 1 \\ j_2 & j_1 & \frac{1}{2} \end{Bmatrix}. \tag{55}$$

The curly bracket denotes the 6-$j$ symbol,[21] and the integral is

$$I_0 = \int_0^\infty v_{l_p j_p}(r) r v_{l_h j_h}(r)\, dr. \tag{56}$$

Following Lemmer and Shakin,[20] we define the form factors for the doorways,

$$f_{c,d}(r) = \langle r, c | V | \phi_d \rangle. \tag{57}$$

Also it is useful to define

$$f_{c,\gamma}(r) = (ik_\gamma)^{-1}\langle r, c | D_\gamma(\mu) | 0 \rangle. \tag{58}$$

Recalling Eqs. (50) and (54), we find that the form factors may be obtained from the following *unprojected form factors*,

$$\langle r, c | V | \phi_d \rangle = C^{\frac{1}{2}\frac{1}{2}T}_{\frac{1}{2}-\frac{1}{2}0}\sum_{j_p' j_h'} C^d_{j_p' j_h'} M(j_p j_h j_p' j_h') r^{-3}$$
$$\times[v_{l_h j_h}(r) v_{l_p' j_p'}(r) v_{l_h' j_h'}(r)], \tag{59}$$

where the $C^d_{j_p' j_h'}$ are the expansion coefficients of doorways,

$$|\phi_d\rangle = \sum_{j_p', j_h'} C^d_{j_p' j_h'} | j_p' j_h'^{-1} JT \rangle, \tag{60}$$

and

$$\langle r, c | D_\gamma(\mu) | 0 \rangle = C^{\frac{1}{2}\frac{1}{2}T}_{\frac{1}{2}-\frac{1}{2}0} N_{ph} v_{l_h j_h}(r), \tag{61}$$

if use is made of Eq. (36). The Clebsch-Gordan coefficients in Eqs. (59) and (61) account for the coupling and the recoupling of the channels in the isospin space. Their appearance is due to the fact that we do not couple the continuum states to good isospin.

Examples of the application of the form factors are seen in the expressions for the following

matrix elements:

$$\langle \phi_d | HG^{(+)}H | \phi_{d'} \rangle = \sum_c \int\int dr\, r f_{c,d}(r) g^{(+)}_{c,E}(r) \times f_{c,d'}(r') r' dr' , \quad (62)$$

and

$$\langle \psi_0^{(-)} | D_\gamma(\mu) | 0 \rangle = i k_\gamma e^{i\delta_{lj}} \int_0^\infty v_{l_p j_p}(r) f_{c,\gamma}(r) r dr . \quad (63)$$

The form factors, Eq. (57), we have defined differ from those of Lemmer and Shakin[20] by the projection prescribed by Eq. (36), which was necessary to make our channel vectors orthogonal to the bound orbitals.

### C. Secondary-Doorway Space

We now have to construct the secondary doorways and evaluate their couplings to the doorways. Because of the shell structure of the nucleus under study, the secondary doorways are chosen to be 3p-3h states. The construction of such complicated states in a microscopic theory is usually prohibitively complicated. For our calculation we find the IBA[13] quite useful. It provides us a systematic construction of higher particle-hole states, taking into account various residual interactions. For doorway–secondary-doorway interactions, we have to further extend the IBA to include the "recoupling" interactions, which were also discussed by Iachello.[13]

In the IBA, we use the idea that a particle-hole pair behaves like a boson. The higher particle-hole states are then considered as multiboson states correlated with residual interactions. For a detailed description, one should refer to the original work.[13] In the following we shall present a simplified version of the approximation. For example, we shall not consider particle-hole and other complicated boson-boson interactions (see Fig. 1).

We first define a *noninteracting* three-boson state as a coupled product of three one-boson states. We may write the noninteracting three-boson state $|\tilde{\Phi}_q\rangle$ as

$$|\tilde{\Phi}_q\rangle = |(B_{12})(B_{34})J_0T_0(B_{56})JT\rangle , \quad (64)$$

where the bosons $|B_{12}\rangle$ (of angular momentum $J_{12}$ and isospin $T_{12}$) and $|B_{34}\rangle$ are coupled to intermediate angular momentum $J_0$ and isospin $T_0$; $J_0$ and $T_0$ are then coupled to the third boson $|B_{56}\rangle$, as shown in Fig. 1. Each boson state is a linear superposition of particle-hole states, as obtained in the TDA (see Sec. III B). With the above notation, we may write

$$|B_{12}\rangle = \sum_{m,n} C^{12}_{mn} |j_m j_n^{-1} J_{12} T_{12}\rangle \quad (65)$$

etc. The unperturbed energy of the (noninteracting) three-boson state, $\tilde{E}_q$, is simply the sum of the boson energies; i.e.,

$$\tilde{E}_q = E_{12} + E_{34} + E_{56} , \quad (66)$$

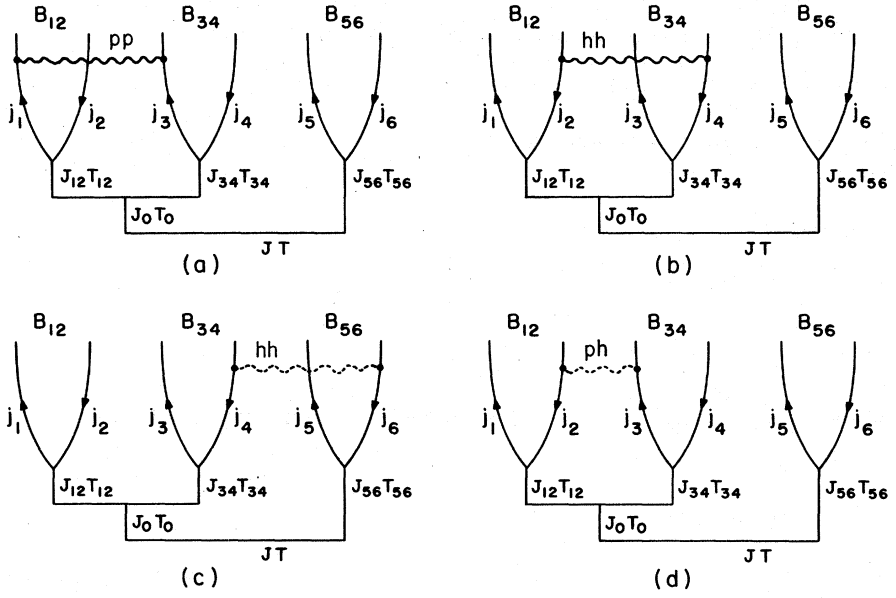


FIG. 1. Boson-boson interactions: We consider only (a) the particle-particle and (b) the hole-hole interactions which involve minimum recouplings. The wavy lines represent interactions between bosons. The sum of interactions (a) and (b) is given by Eq. (70). Other *recoupling* interactions, such as (c) and (d), are neglected in our formulation.

where $E_{12}$ is the energy of the boson state $|B_{12}\rangle$ etc.

The degeneracy of the three-boson states may be removed if we allow these bosons to interact with each other. The boson-boson interaction may be of particle-particle (pp), hole-hole (hh), and particle-hole (ph) type, as shown in Fig. 1. Within our approximation, we assume that only the pp and the hh interactions are important. We also take into account only the pp and hh interactions which involve *minimum* recoupling of angular momentum; these interactions are shown by the wavy lines in Fig. 1. We have neglected any ph interaction *between* bosons and more complicated "recoupling" pp and hh interactions. Some of these neglected interactions are also shown by the dashed lines in Fig. 1.

In order to evaluate these pp and hh interactions, it is convenient to introduce a pp and hh matrix element between two 3p-3h configurations. We may write a 3p-3h configuration $|\beta\rangle$, for example,

as

$$|\beta\rangle = |(j_1 j_2^{-1})J_{12}T_{12}(j_3 j_4^{-1})J_{34}T_{34}; J_0 T_0 (j_5 j_6^{-1})J_{56}T_{56}JT\rangle\,, \tag{67}$$

and $|\beta'\rangle$ for the state with all the quantities primed. For simplicity, a *noninteracting* three-boson state may be written as

$$|\tilde{\Phi}_q\rangle = \sum_\beta C_\beta^q |\beta\rangle\,. \tag{68}$$

We now denote the pp and hh interactions between configurations $|\beta\rangle$ and $|\beta'\rangle$ which involve minimum recoupling as,

$$I_{\rm pp}^{\rm hh}(\beta', \beta) = \langle\beta'|V|\beta\rangle_{\rm pp\ and\ hh\ only}\,. \tag{69}$$

This quantity has been given by Iachello,[13] incorporating the isospin variables, as

$$\begin{aligned} I_{\rm pp}^{\rm hh}(\beta', \beta') &= \delta_{J_0 J_0'}\delta_{T_0 T_0'}\Delta_{j_5 j_6, j_5' j_6'} A_{12,34}^{JT} \\ &\times \sum_{J_s, J_s', T_s, T_s'} [J_s, T_s][J_s', T_s'] \begin{Bmatrix} j_1 & j_2 & J_{12} \\ j_3 & j_4 & J_{34} \\ J_s & J_s' & J_0 \end{Bmatrix} \begin{Bmatrix} j_1' & j_2' & J_{12}' \\ j_3' & j_4' & J_{34}' \\ J_s & J_s' & J_0 \end{Bmatrix} \begin{Bmatrix} \frac{1}{2} & \frac{1}{2} & T_{12} \\ \frac{1}{2} & \frac{1}{2} & T_{34} \\ T_s & T_s' & T_0 \end{Bmatrix} \begin{Bmatrix} \frac{1}{2} & \frac{1}{2} & T_{12}' \\ \frac{1}{2} & \frac{1}{2} & T_{34}' \\ T_s & T_s' & T_0 \end{Bmatrix} \\ &\times [G(j_2 j_4 j_2' j_4' J_s' T_s')\Omega(j_1 j_3 j_1' j_3' J_s T_s) + G(j_1' j_3' j_1 j_3 J_s T_s)\Omega(j_2 j_4 j_2' j_4' J_s' T_s')]\,, \end{aligned} \tag{70}$$

where we have defined $[J, T] \equiv (2J+1)(2T+1)$. The curly brackets are the 9-$j$ symbols. The $G$'s are the antisymmetrized two-particle matrix elements as defined by (see Ref. 20)

$$G(j_a j_b j_c j_d JT) = (j_a j_b JT|V|j_c j_d JT) - (-)^{j_c + j_d + J + 1 + T}(j_a j_b JT|V|j_d j_c JT)\,, \tag{71}$$

where $(j_a j_b JT|V|j_c j_d JT)$ are the unsymmetrized two-particle matrix elements. The other symbols in Eq. (70) are defined as

$$\Delta_{j_5 j_6, j_5' j_6'} = \delta_{j_5 j_5'}\delta_{j_6 j_6'}\delta_{J_{56} J_{56}'}\delta_{T_{56} T_{56}'}\,, \tag{72}$$

$$A_{12,34}^{JT} = ([J_{12}, T_{12}][J_{34}, T_{34}][J_{12}', T_{12}'][J_{34}', T_{34}'])^{1/2}\,, \tag{73}$$

and

$$\Omega(j_a j_b j_a' j_b' J_s T_s) = \delta_{j_a j_a'}\delta_{j_b j_b'} - (-)^{j_a + j_b + J_s + 1 + T_s}\delta_{j_a j_b'}\delta_{j_a' j_b}\,. \tag{74}$$

In our applications, we may simplify Eq. (70) by imposing the following conditions:

$$T_{12} = T_{12}' = T_{34} = T_{34}' = T_0 = T_0' = 0\,. \tag{75}$$

Equation (70) can then be reduced to

$$\begin{aligned} I_{\rm pp}^{\rm hh}(\beta', \beta) &= \tfrac{1}{4}\delta_{J_0 J_0'}\delta_{T_0 T_0'}\Delta_{j_5 j_6, j_5' j_6'}([J_{12}, J_{34}][J_{12}', J_{34}'])^{1/2} \sum_{J_s, J_s', T_s} [J_s][J_s'][T_s] \begin{Bmatrix} j_1 & j_2 & J_{12} \\ j_3 & j_4 & J_{34} \\ J_s & J_s' & J_0 \end{Bmatrix} \begin{Bmatrix} j_1' & j_2' & J_{12}' \\ j_3' & j_4' & J_{34} \\ J_s & J_s' & J_0 \end{Bmatrix} \\ &\times [G(j_2 j_4 j_2' j_4' J_s' T_s)\Omega(j_1 j_3 j_1' j_3' J_s T_s) + G(j_1' j_3' j_1 j_3 J_s T_s)\Omega(j_2 j_4 j_2' j_4' J_s' T_s)]\,, \end{aligned} \tag{76}$$

which we have used in our calculation.

Several remarks are in order in connection with the above particle-particle and hole-hole correlations.

(1) If we neglect the recoupling terms, that is if we use Eq. (76) in the 3p-3h configuration [Eq. (67)], the pp and hh interactions are identical to those in a 2p-2h configuration,

$$|(j_1 j_2^{-1})J_{12}T_{12}(j_3 j_4^{-1})J_{34}T_{34};J_0T_0\rangle .$$

That is, the pp and hh interactions are calculated only between the first two bosons in this coupling scheme.

(2) The $I_{pp}^{hh}$ generally contain off-diagonal matrix elements in the representation of Eq. (64). The new (interacting) three-boson states, $|\Phi_q\rangle$, would be linear combinations of the $|\tilde{\Phi}_q\rangle$, after the diagonalization of pp and hh interactions.

(3) We have neglected the Pauli principle, and the problems associated with nonorthogonal basis vectors in the construction of the three-boson states.

The first remark shows that the expression Eq. (76) can be directly used to calculate, at no extra cost, the pp and hh correlations in a two-boson state $|(B_{12})(B_{34})J_0T_0\rangle$. If the off-diagonal $I_{pp}^{hh}$ terms are small, we may use the first-order perturbation to obtain the energies of the three-boson states $|\phi_q\rangle$ as

$$E_q = \tilde{E}_q + \sum_{\beta',\beta} C_\beta^q C_{\beta'}^q I_{pp}^{hh}(\beta',\beta) . \tag{77}$$

In this case the boson picture becomes even simpler. The noninteracting bosons are shifted by, but *not mixed* by, the pp and hh interactions. We should also note that these shifts may be quite large even if the mixing due to off-diagonal elements is small. The effects of the Pauli principle cannot be easily taken into account. We simply hope that these are small and thus can be neglected. Further discussion may be found in Ref. 13.

### D. Doorway-Secondary-Doorway Coupling

After we have constructed the doorways and the secondary doorways, we need the coupling matrix elements between these two sets of states. Let us denote the matrix elements between a 1p-1h configuration, $|(j_1' j_2'^{-1})JT\rangle$, denoted by $\alpha$, and a 3p-3h configuration, denoted by $\beta$, in Eq. (67) as

$$V_{\alpha\beta} = \langle (j_1' j_2'^{-1})JT\,|\,V\,|\,(j_1 j_2^{-1})J_{12}T_{12}(j_3 j_4^{-1})J_{34}T_{34};J_0T_0(j_5 j_6^{-1})J_{56}T_{56}JT\rangle . \tag{78}$$

The interaction between $\phi_d$ and $\phi_q$ can then be written as

$$\langle \phi_d | H_{dq} | \phi_q \rangle = \sum_{\alpha,\beta} C_\alpha^d C_\beta^q V_{\alpha\beta} , \tag{79}$$

where $C_\alpha^d$ and $C_\beta^q$ are the configuration-mixing coefficients of the doorways and the secondary doorways. Here $\alpha$ and $\beta$ denote all the quantum numbers necessary to specify the configurations.

The simplest interaction in $V_{\alpha\beta}$ is the nonrecoupling term, as shown diagrammatically in Fig. 2. This term has been evaluated by Iachello to be[13]

$$L_{12,34}^{56} = ([J_{12}][T_{12}])^{1/2}(-)^{j_3+j_4+J_{12}+T_{12}}\delta_{J_0 0}\delta_{T_0 0} \times \Delta_{j_5 j_6, j_1' j_2'}\langle (j_4 j_3^{-1})J_{12}T_{12}\,|\,V\,|\,(j_1 j_2^{-1})J_{12}T_{12}\rangle . \tag{80}$$

This term will be called the *reference term* in our discussion. It describes the annihilation of the 1p-1h pairs (12, 34); the third particle-hole pair moves independently and becomes the final state, $|(j_1' j_2'^{-1})JT\rangle$, as in Fig. 2.

There are two other such simple terms,[24] which do not involve any recoupling of the particle-hole pairs used to define each boson of the three-boson states (Fig. 2). The contribution of these simple terms to Eq. (77) vanishes identically if the one-boson states comprising the three-boson state; i.e., $|B_{12}\rangle$, $|B_{34}\rangle$, and $|B_{56}\rangle$, are each orthogonal to the final doorway (one-boson) state. Such a situation occurs in our application. We therefore have to look for contributions from more complicated interaction terms. As shown in Eq. (80), the reference term (and other simple terms) involves a particle-hole pair annihilation interaction which does not depend on the particle-hole states in one of the bosons. There are, however, more complicated interaction terms where *all* the three bosons are involved. We show one example of such terms in Fig. 3. For simplicity we may call these terms which involve "breaking up" the bosons, *the recoupling terms*.

There are six such recoupling terms. They can all be related to the reference term by unitary transformations. For simplicity, we shall always restrict ourselves to Eq. (75). The six recoupling terms are given in Table II. Diagrammatically we illustrate the first recoupling term in Fig. 3. For detailed derivation of these terms, one is referred to Appendix B and Ref. 24.

The doorway–secondary-doorway coupling may

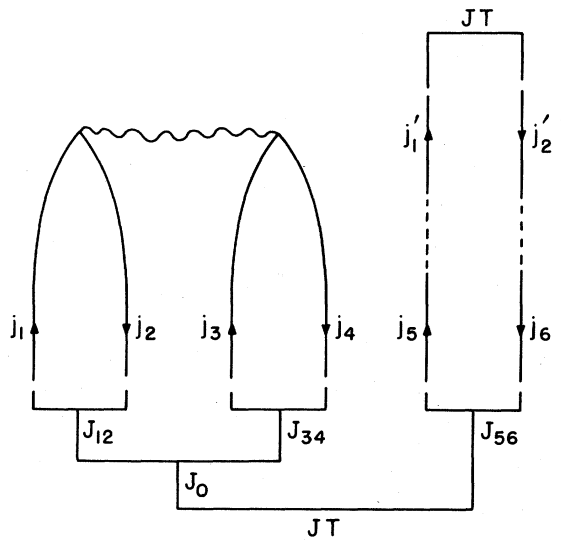


FIG. 2. The nonrecoupling term in the doorway–secondary-doorway interaction. One particle-hole pair $|j_5 j_6^{-1} J_{56}\rangle$ moves freely and the other two pairs are annihilated. The analytic expression for this diagram is given by Eq. (80).

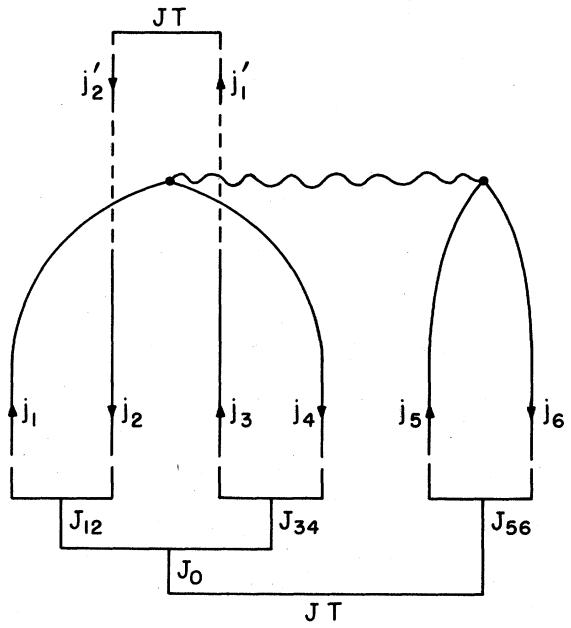


FIG. 3. A typical recoupling term. The analytic expression for this term is given as $R(1)$ in Table II, and is expressed there in terms of the reference term of Eq. (80).

then be written as

$$\langle \phi_d | H_{dq} | \phi_q \rangle = \sum_{\alpha,\beta} \sum_{k=1}^{6} C_\alpha^d C_\beta^q [R(k)]_{\alpha\beta} , \tag{81}$$

where $R(k)$ are given in Table II, in terms of the notations defined in Eqs. (80) and (78).

We have now obtained all the shell-model formulation necessary to calculate the $T$ matrix and therefore the cross sections of our interest. It is, however, also interesting to study the other nuclear-structure aspects of the calculation. With the matrix elements, Eq. (81), we may diagonalize the energy matrix and obtain the *compound states* $|\Phi_D\rangle$ as

$$|\Phi_D\rangle = \sum_d C_d^D |\phi_d\rangle + \sum_q C_q^D |\phi_q\rangle , \tag{82}$$

where $C_d^D$ and $C_q^D$ are the configuration-mixing coefficients. (See Table VIII.)

## IV. NUMERICAL RESULTS

In this section we shall present the results of

TABLE II. Recoupling terms $R(k)$ [see Eq. (81)].

| | |
|---|---|
| $R(1)$ | $(-)^{j_1+j_3+J_{12}+J_0+J_{56}} \frac{1}{\sqrt{12}} ([J_{12}][J_{34}][J_0])^{1/2} \begin{Bmatrix} j_2 & j_1 & J_{12} \\ j_3 & j_4 & J_{34} \\ J & J_{56} & J_0 \end{Bmatrix} L^{32}_{14,56}$ |
| $R(2)$ | $(-)^{j_2+j_4+J_{34}+J_0+J} \frac{1}{\sqrt{12}} ([J_{12}][J_{34}][J_0])^{1/2} \begin{Bmatrix} j_1 & j_2 & J_{12} \\ j_4 & j_3 & J_{34} \\ J & J_{56} & J_0 \end{Bmatrix} L^{14}_{32,56}$ |
| $R(3)$ | $(-)^{j_4+j_6+J_{34}+1+J} \frac{1}{\sqrt{12}} ([J_{34}][J_{56}][J_0])^{1/2} \begin{Bmatrix} j_3 & j_6 & J \\ J_{56} & J_0 & j_5 \end{Bmatrix} \begin{Bmatrix} j_4 & j_5 & J_{12} \\ J_0 & J_{34} & j_3 \end{Bmatrix} L^{36}_{12,54}$ |
| $R(4)$ | $(-)^{j_1+j_5+J_{12}+J_{56}+1+J_0} \frac{1}{\sqrt{12}} ([J_{12}][J_{56}][J_0])^{1/2} \begin{Bmatrix} j_2 & j_5 & J \\ J_{56} & J_0 & j_6 \end{Bmatrix} \begin{Bmatrix} j_1 & j_6 & J_{34} \\ J_0 & J_{12} & j_2 \end{Bmatrix} L^{52}_{16,34}$ |
| $R(5)$ | $(-)^{j_3+j_5+J_{12}+J_{56}+1} \frac{1}{\sqrt{12}} ([J_{34}][J_{56}][J_0])^{1/2} \begin{Bmatrix} j_6 & j_3 & J_{12} \\ J_{34} & J_0 & j_4 \end{Bmatrix} \begin{Bmatrix} j_5 & j_4 & J \\ J_0 & J_{56} & j_6 \end{Bmatrix} L^{54}_{12,36}$ |
| $R(6)$ | $(-)^{j_2+j_6+J_{34}+J_0+1+J} \frac{1}{\sqrt{12}} ([J_{12}][J_{56}][J_0])^{1/2} \begin{Bmatrix} j_1 & j_6 & J \\ J_{56} & J_0 & j_5 \end{Bmatrix} \begin{Bmatrix} j_2 & j_5 & J_{34} \\ J_0 & J_{12} & j_1 \end{Bmatrix} L^{16}_{52,34}$ |

calculations based on the shell-model formulation described above. We begin with a schematic of the low-lying 1p-1h one-boson states of $O^{16}$ shown in Fig. 4, including some of the 3p-3h states, which we calculate as being in the giant-dipole region (20–26 MeV). We are primarily interested in the photonuclear excitation from the ground state to the compound states (in the dipole region) and their subsequent decay by proton or neutron emissions. We consider the channels in which the residual nucleus may be in the ground state ($J^\pi = \frac{1}{2}^-$) or the third excited state ($J = \frac{3}{2}^-$); these states are believed to be predominantly represented by simple one-hole configurations.[25] The positive-parity low-lying excited states of $O^{15}$ or $N^{15}$ are neglected in the present calculation, their structure being more complicated, probably containing 1p-2h configurations. The effects of the neglected channels are parametrized in terms of the quantities $\Gamma_q$ and $\Gamma_X$, as discussed previously; $\Delta_q$ and $\Delta_X$ are neglected.

We choose a local, real Woods-Saxon potential to define our single-particle basis. We need the neutron-particle states (with energy given in MeV):

$$1d_{5/2}\ (-4.14),\quad 2s_{1/2}\ (-3.27),\quad \text{and } 1d_{3/2}\ (0.93),$$

where the $1d_{3/2}$ state is the single-particle resonance, and the neutron hole states,

$$1p_{3/2}\ (-21.84) \text{ and } 1p_{1/2}\ (-15.67).$$

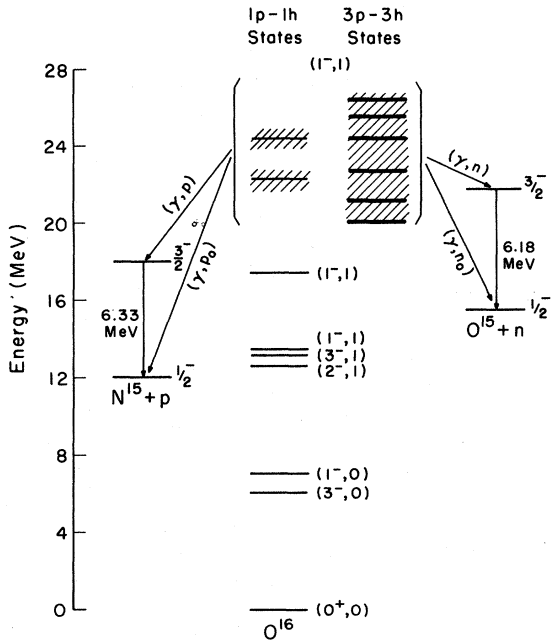


FIG. 4. Some energy levels of $O^{16}$ and the decay modes of the giant dipole resonances as considered in our formulation. Some 3p-3h states, constructed in our calculation, are shown as being in the dipole region.

The corresponding proton levels are about 3.5 MeV higher because of the Coulomb forces. The parameters for the Woods-Saxon potentials are chosen to reproduce the bound-state energy or the single-particle resonance energy. (The potentials are chosen to be independent of the states of the residual nucleus.) The parameters are given in Ref. 24, they are close to those used by Perez and MacDonald.[1]

Owing to the presence of the $d_{3/2}$ single-particle resonance at $E_R = 0.93$ MeV, we have to redefine our $P$ space as prescribed in Ref. 19. Following the procedure outlined in this reference, we define the "resonance wave packet" $\phi_R(r)$ as

$$\phi_R(r) = \kappa v_{d_{3/2},\,E_R}(r), \quad r < R$$
$$= 0, \quad r \geq R, \tag{83}$$

where $v_{d_{3/2},\,E_R}(r)$ is the continuum wave function at the resonance energy $E_R$, $\kappa$ is a normalization factor, and $R$ a cutoff radius. As a supplement to Ref. 19, we show the effect of changing the cutoff radius on the $d_{3/2}$ potential scattering cross section for various energies in Table III. We demonstrate that the projection procedure[19] is not sensitive to $R$, within a reasonable range of values. We take $R = 8.0$ fm. The resonance wave packet, $\phi_R$, is then to be considered on the same footing as a bound orbital (see Ref. 19).

The basic 1p-1h configurations, used for both protons and neutrons, of our doorway space are

$$d_{3/2}p_{3/2}^{-1}\ (22.77\text{ MeV}),\quad s_{1/2}p_{3/2}^{-1}\ (18.57\text{ MeV}),$$
$$d_{5/2}p_{3/2}^{-1}\ (17.70\text{ MeV}),\quad d_{3/2}p_{1/2}^{-1}\ (16.64\text{ MeV}),$$
$$s_{1/2}p_{1/2}^{-1}\ (12.40\text{ MeV}),\quad d_{5/2}p_{1/2}^{-1}\ (11.53\text{ MeV}).$$

These configurations are mixed through the residual interactions. Such calculations are familiar[20,26] and we shall not discuss the complete calculation here. The residual interaction is taken to be the zero-range limit of the Soper mixture;

TABLE III. Effects of the cutoff radius on the modification of the single-particle potential scattering cross-section (in barns) ($d_{3/2}$ partial wave only).

| Cutoff radius (fm) | Energy (MeV) 0.943 | 1.04 | 1.14 | 1.24 | 1.34 |
|---|---|---|---|---|---|
| 9.6 | 0.019 | 0.005 | 0.007 | 0.008 | 0.01 |
| 6.4 | 0.0001 | 0.0059 | 0.0076 | 0.0091 | 0.0112 |
| 4.5 | 0.013 | 0.018 | 0.0218 | 0.0259 | 0.031 |
| 3.2 | 0.068 | 0.070 | 0.08 | 0.0903 | 0.099 |
| 1.9 | 0.665 | 0.63 | 0.46 | 0.098 | 0.56 |
| Unmodified cross section (b) | 5.24 | 1.03 | 0.46 | 0.30 | 0.23 |

that is, we take ($b = 1.76$ fm),

$$V_{ij} = -582.3(\pi_t + 0.46\pi_s)\delta(\vec{r}_i - \vec{r}_j)\ \text{MeV fm}^3 . \tag{84}$$

We list those 1p-1h states which enter our later discussions in Table IV. The states at 24.45 and 22.31 MeV contain 27.5 and 65% of the total dipole strengths, respectively.[27] They are the "giant-dipole states" and are therefore identified as our doorway states. The projected and the unprojected form factors for these two doorways are shown in Figs. 5 and 6, for all the channels included in our calculation.

Using the form factors, we may now calculate the continuum mixing of the doorways. The widths and the shifts will be smooth functions of energy, if single-particle resonances are removed from the $P$ space. For example, we show the modification of the continuum shifts due to the removal of the $d_{3/2}$ resonance from the $P$ space in Table V. We see that resonance behavior at about 1 MeV is completely removed. (The effects of single-particle resonances on the importance of channel-channel coupling was also discussed in Ref. 20.)

The gross structure of the dipole resonance can then be easily reproduced in our formulation by setting $W_d^{\downarrow} = 0$ in the $T$ matrix. For illustration we show the gross structure of the $(\gamma, n_0)$ cross section in Fig. 7. It is interesting to see that our $T$ matrix with $W_d^{\downarrow} = 0$ and $\Gamma_X = 700$ keV gives a cross section quite similar to that obtained by Buck and Hill.[1] The result, however, falls into the same epilog: The dipole strength is much too concentrated and no account can be given of the

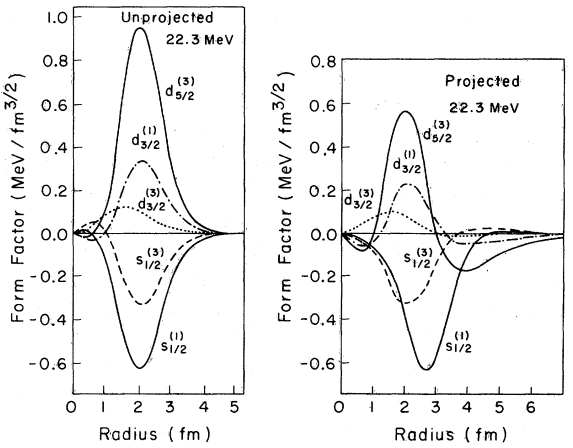


FIG. 5. The projected and the unprojected form factors, Eqs. (57) and (59), of the 22.3-MeV doorway in various channels. The superscript refers to the final channel; (1) refers to the $p_{1/2}{}^{-1}$ channel and (3) to the $p_{3/2}{}^{-1}$ channel.

intermediate structure. For this reason, it is natural to search for an extension of the doorway calculation to include more complicated configurations.[6-8] In our formulation, such complicated configurations are the secondary doorways which in $O^{16}$ are 3p-3h states. We may now turn to the consideration of the 3p-3h states which may exist in the dipole region.

In the IBA, the 3p-3h states may be considered as composed of three bosons interacting through residual boson-boson interactions. First of all we have to find our elementary bosons, which will be considered as the building blocks for multi-boson states. Here we return to Fig. 4 and Table

TABLE IV. One-particle–one-hole configuration mixing coefficients.

| $(J^\pi T)$ | Energy (MeV) | $(s_{1/2}p_{3/2}{}^{-1})$ | $(d_{5/2}p_{3/2}{}^{-1})$ | $(d_{3/2}p_{3/2}{}^{-1})$ | $(d_{3/2}p_{1/2}{}^{-1})$ | $(s_{1/2}p_{1/2}{}^{-1})$ | $(d_{5/2}p_{1/2}{}^{-1})$ |
|---|---|---|---|---|---|---|---|
| | | | Giant-dipole states | | | | |
| $(1^-1)$ | 24.45 | −0.0607 | −0.0740 | 0.9714 | −0.2173 | 0.0021 | |
| $(1^-1)$ | 22.31 | 0.1225 | 0.9345 | 0.1452 | 0.2973 | 0.0483 | |
| | | | One-boson states | | | | |
| $(1^-1)$ | 17.43 | −0.0539 | −0.3160 | 0.1806 | 0.9297 | −0.0162 | |
| $(1^-1)$ | 13.48 | −0.0507 | −0.0440 | −0.0084 | 0.0011 | 0.9977 | |
| $(2^-1)$ | 12.66 | 0.0243 | 0.2020 | 0.0530 | 0.0164 | | 0.9775 |
| $(3^-1)$ | 13.18 | | −0.2210 | 0.0064 | | | 0.9753 |
| $(1^-0)$ | 11.32 (7.1) [a] | 0.2199 | −0.2221 | 0.0344 | −0.1688 | 0.9342 | |
| $(1^-0)$ | 8.89 (spurious) | 0.1400 | 0.7608 | −0.1441 | 0.5621 | 0.2548 | |
| $(3^-0)$ | 8.78 (6.1) [a] | | 0.2719 | −0.1974 | | | 0.9419 |

[a] Energies in parentheses are experimental values (see Sec. V).

IV, where a boson is denoted by its $J^\pi T$ value (later by just $JT$ in our discussion). They are obtained in the TDA. By comparing the energies of these bosons (Table IV) with the experimental values (Fig. 4), we find that $T=1$ states are quite well described by TDA. The $T=0$ states are more complicated for several reasons. First, we have the contamination of the spurious state which describes the motion of the center of mass. We identify this spurious state as the lowest $J=1^-$, $T=0$ state in our calculation.[26] The lowest relevant $T=0$ states now come out at 11.32 MeV ($J^\pi=1^-$) and 8.89 MeV ($J^\pi=3^-$), while the experiments yield such states at 7.1 and 6.1 MeV, respectively. There are at least two effects we have to consider: The experimental levels are not pure 1p-1h, and we have ignored the ground-state correlations in the calculation. We would expect that the mixing of our $J^\pi=3^-$ state with $T=0$ low-lying 3p-3h states will push its energy downward. Also the consideration of ground-state correlations should also improve the $T=0$ spectrum.[26] We approximate the states observed at the experimental energies with our 1p-1h wave functions of Table IV. The identification of the calculated $J^\pi=1^-$ state at 11.32 MeV with the 7.1-MeV state is probably a poor approximation as the latter state is very likely mainly of 3p-3h character. As we will see, however, the three-boson states which involve our 1p-1h model for the state at 7.1 MeV play an insignificant role in the calculation, since these turn out to be only weakly coupled to the doorway states. The 6.1-MeV ($J^\pi=3^-$) state plays an important role and for this state our model should provide a more adequate description. Our approximation is apparently good if the effects of the ground-state correlations and the admixture of higher configurations are such that they have important effects on the energy spectrum of the low-lying $T=0$ mode, but not on the (coupling) matrix elements.

Before we construct the $J=1^-$, $T=1$ 3p-3h states, we find it instructive to discuss the low-lying, positive-parity, two-boson states of $O^{16}$. We recall that, keeping only the interactions involving the least recoupling, the particle-particle and

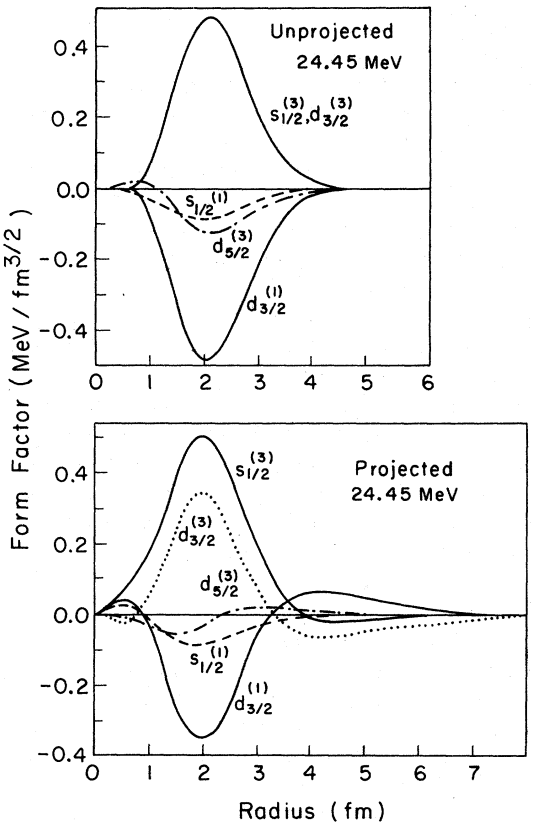


FIG. 6. The projected and the unprojected form factors of the 24.45-MeV doorway in various channels. The superscript refers to the final channel (see caption to Fig. 5).

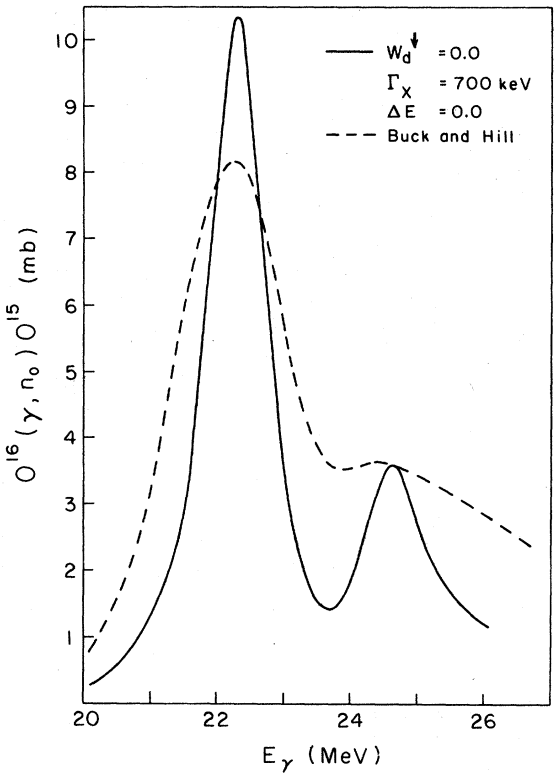


FIG. 7. The doorway-state gross-structure calculation (solid line), which is obtained from our $T$ matrix, Eq. (32), by setting $W_d^{\downarrow}(E)=0$. The quantity $\Gamma_X$ (chosen to be 700 keV) is used as an energy-averaging parameter in the $T$ matrix. The cross section is compared with that of the complex optical-model calculation of Buck and Hill (Ref. 1) (dashed line).

TABLE V. Modification on the continuum mixing of the doorways due to removal of single-particle resonance. The subscripts 1 and 2 refer to the doorways at 24.45 and 22.31 MeV, respectively.

| Neutron continuum shift (MeV) | | Energy in $(d_{3/2}p_{1/2}^{-1})$ channel (MeV) 1.0 | 2.0 | 3.0 | 4.0 | 5.0 |
|---|---|---|---|---|---|---|
| $\Delta_1^{\dagger}(E)$ | Unmodified | 4.65 | 0.434 | 0.217 | 0.142 | 0.105 |
| | Modified | −0.114 | −0.083 | −0.044 | −0.0165 | −0.0037 |
| $\Delta_2^{\dagger}(E)$ | Unmodified | 2.35 | 0.22 | 0.11 | 0.07 | 0.054 |
| | Modified | −0.0565 | −0.041 | −0.021 | −0.007 | −0.0006 |

hole-hole interactions are identical in both 2p-2h and 3p-3h states under our consideration (cf. Sec. III C).

Beginning with the lowest two $T=0$ bosons, we obtain degenerate two-boson states, as shown in Fig. 8. The degeneracy is removed by the p-p and h-h interactions. The matrix elements due to p-p and h-h interactions are shown in Table VI. In Fig. 8, we keep only the first-order perturbation, neglecting the off-diagonal terms of Table VI; the two-boson states are considered unmixed by the p-p and h-h interactions and are only shifted in energy. In Fig. 8, we further notice that the unperturbed two-boson states are perturbed by the p-p and h-h correlations to such an extent that no harmonicity is retained.

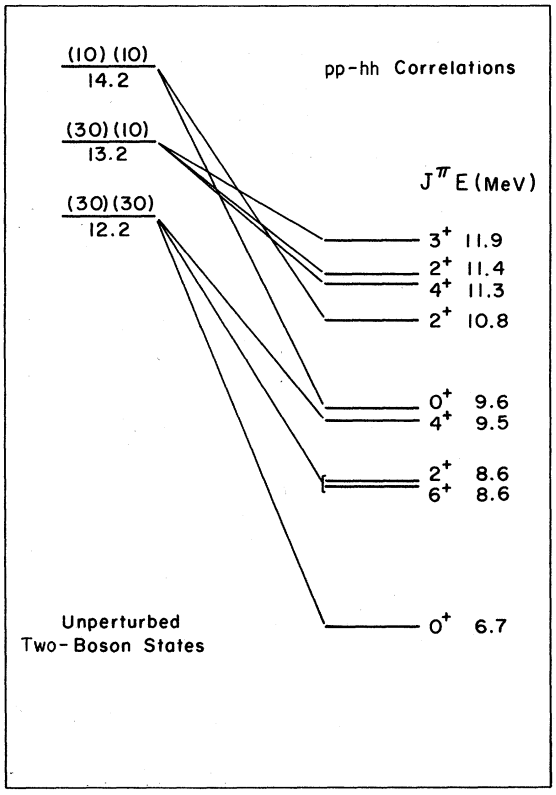


FIG. 8. Effect of the particle-particle and hole-hole interactions in removing the degeneracy of the two-boson states.

It is interesting to point out that we have shown a mechanism for the 2p-2h states to come down in energy without using a deformed state description.[9] The two-boson states are at low energy and their mixing with the ground state becomes important. It is known that the 4p-4h states would also be pushed down in energy and mixed with the 2p-2h states and the ground state to generate the ground-state correlations in $O^{16}$. The structure of the 6.06-MeV $0^+$ state may also be understood in the IBA; a schematic calculation of this kind was performed by Iachello.[13]

We may proceed to construct the 3p-3h states. We denote the odd-parity one-boson states with angular momentum $J$ and isospin $T$ as $(JT)$ – see Table IV. We first couple the two one-boson states, (30) and (10), to some intermediate angular momentum $J_0$, and then couple these two-boson states to (11), (21), and (31) one-boson states. The degenerate spectrum is shown in Fig. 9. Incorporating the p-p and h-h correlations, the spectrum is shifted downward and the degeneracy removed. We have given only the states in the dipole region, there being many higher states. We emphasize once again that the general belief that the 3p-3h states will be above the dipole region is because of the neglect of the strong p-p and h-h interactions. We have now demonstrated the truth of our first crucial assumption: There are 3p-3h states in the dipole region.

We next turn to the question: Are these 3p-3h states coupled to the giant-dipole states with appropriate strengths? Since the "nonrecoupling" interactions vanish, we expect small coupling strengths from the "recoupling" terms. Keeping in mind that we were able to reproduce the gross structure by doorway calculations, we hope to find only a *few* secondary doorways with strong coupling, just enough to reproduce the distinct peaks in the cross section. We show the result of our calculation in Table VII. Indeed there are only a few states with strong coupling; they are

also distinct in energy. Whether these coupling matrix elements are of "correct" magnitude can only be tested in a complete calculation of the $T$ matrix; the relative size of the peaks in the cross sections are *very* sensitive to these values.

A *trial* calculation with the matrix elements as given in Table VII and the parameters,

$$\Delta_q = \Delta_X = 0,$$

and

$$\Gamma_q = \Gamma_X = 400 \text{ keV}, \tag{85}$$

gives the "intermediate structure" shown in Fig. 10. By comparison with the experiment, we realize that both the resonance energies and the relative strengths are not correctly reproduced, although they have successfully reproduced some structure. Apparently the 3p-3h states are coupled too strongly to the main peak at 22.3 MeV and the energy of some state near 24 MeV needs to be adjusted.

To introduce the necessary adjustments, let us first recapitulate the approximations we have made in the energies and the couplings of these 3p-3h states. The residual interaction, first of all, is only a crude approximation of the nucleon-nucleon interaction. Furthermore, we have calculated the energies by including only the simplest terms of the p-p and h-h interactions. There are other smaller contributions from more complex recoupling terms, including some recoupling p-h interactions. We have also completely neglected the problems associated with the Pauli principle (the blocking effect) and the nonorthogonality of our 3p-3h basis. In addition to the uncertainties in the boson energies, the quantities $\Delta_X$ and $\Delta_q$ also affect the energies in Eq. (32). The force we have used and the approximate nature of the wave functions, of course, provide us only with approximate coupling strengths.

TABLE VI. Particle-particle and hole-hole interactions in two-boson states (MeV).

| Configuration | (30)(30)$J$ | (30)(10)$J$ | (10)(10)$J$ |
|---|---|---|---|
| $J=0$ | | | |
| (30)(30)$J$ | −5.524 | | |
| (10)(10)$J$ | −0.886 | | −4.624 |
| $J=2$ | | | |
| (30)(30)$J$ | −3.6 | | |
| (30)(10)$J$ | −0.026 | −1.83 | |
| (10)(10)$J$ | −0.34 | 0.43 | −3.41 |
| $J=4$ | | | |
| (30)(30)$J$ | −2.74 | −0.185 | |
| (30)(10)$J$ | −0.185 | −1.92 | |
| $J=3$ | | | |
| (30)(10)$J$ | | −1.34 | |
| $J=6$ | | | |
| (30)(30)$J$ | −3.63 | | |

We therefore judge ourselves at liberty to make the following modifications: (i) We adjust the energies of two strongly coupled states as shown in Table VIII, and (ii) we reduce all the coupling matrix elements to the doorway at 22.3 MeV by 15%. The weakly coupled states are not shifted; they affect the final calculations only in a minor way. These adjustments should be deemed as minor and well within the approximation.

We may now recalculate the cross section with the adjusted spectrum and coupling strengths. First we have to define an intermediate-resolution cross section. This can be done by choosing appropriate values for $\Gamma_q$ and $\Gamma_X$ to reproduce the integrated cross section. With the parameters given by Eq. (85), we have the intermediate-resolution cross section $\sigma_I(\gamma, n_0)$ satisfying

$$\int_{20.5\text{ MeV}}^{26\text{ MeV}} \sigma_I(\gamma, n_0) dE = 17.0 \text{ mb MeV}, \tag{86}$$

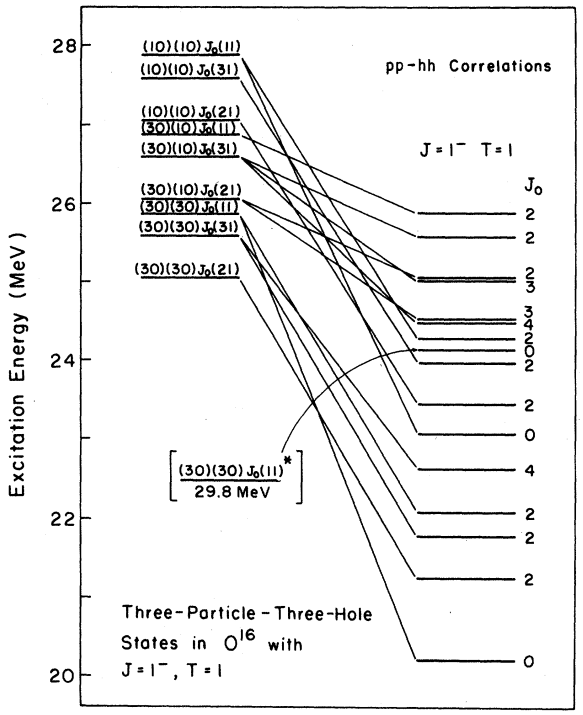


FIG. 9. Effect of the particle-particle and hole-hole interactions in removing the degeneracy of the three-boson states. The intermediate angular momentum of two-boson states is denoted by $J_0$. The state denoted (11)* is at 17.43 MeV (see Tables IV and VII), and the state (30)(30) $J_0$ (11)* has an unperturbed energy of 29.8 MeV.

which is close to the experimental value.[28] We have taken $\Gamma_q$ and $\Gamma_X$ to be constant for simplicity. They are generally energy-dependent as discussed in Appendix A. We have used the ground-state cross section $\sigma(\gamma, n_0)$ as our reference, since it is better determined experimentally. The compound shifts and widths are shown in Fig. 11, with $\Gamma_q$ = 400 keV. The intermediate-resolution cross section and its energy average with $\Delta E$ = 200 keV are shown in Fig. 12. The agreement with the experiment[28] is excellent. We have completely reproduced the intermediate structure, including the resonance energies and the relative strengths.[29]

In order to obtain further nuclear-structure information in the giant-dipole region, we may diagonalize the energy matrix of the one- and three-boson states. Such diagonalization provides us with the resonance energies of the compound states and their microscopic structure in terms of the interacting bosons. We show the results in Table VIII and Fig. 13. In Table VIII, we include only nine secondary-doorway states which are mixed appreciably with the dipole states; others are not mixed, and are therefore not shifted in energy. After the diagonalization, we list five compound states, each containing appreciable 1p-1h admixture. These compound states are shown in Table VIII. [Two other states at 21.73 and 25.60 MeV also contain some dipole strength (see Table IX).] Many states fail to attain any dipole character,

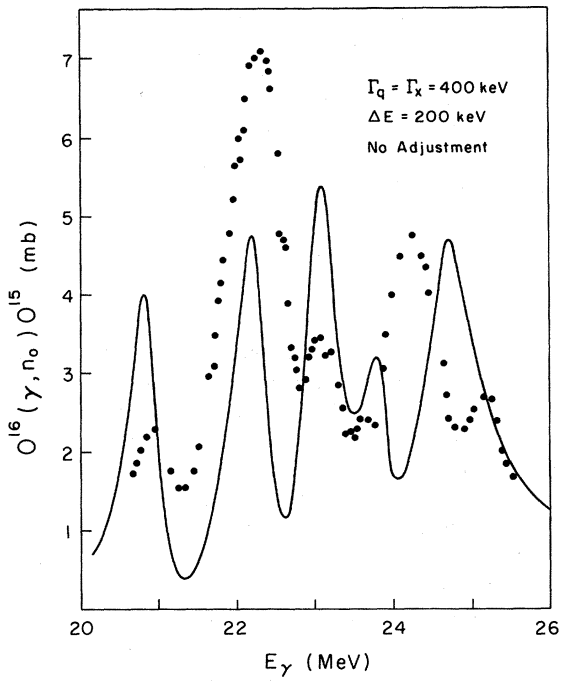


FIG. 10. The intermediate structure as obtained without adjustments in the secondary-doorway energies and their couplings to the doorways is shown. We note that the strength at 22.3 MeV is shifted too much by the coupling and the energies of the intermediate resonances are not correctly reproduced. The experimental data are taken from Caldwell *et al.*, (Ref. 3).

TABLE VII. Spectrum of the secondary-doorway states and the coupling strengths.

| Energy (MeV) | Configuration | Coupling matrix element to the doorway at 22.31 MeV (MeV) | 24.45 MeV (MeV) |
|---|---|---|---|
| 25.88 | (30)(10)2(11) | 0.025 | 0.000 |
| 25.58 | (30)(10)2(31) | 0.224 | −0.057 |
| 25.06 | (30)(10)2(21) | 0.132 | −0.041 |
| 25.05 | (30)(10)3(31) | 0.003 | 0.016 |
| 24.53 | (30)(10)3(21) | −0.104 | −0.002 |
| 24.48 | (30)(10)4(31) | 0.091 | −0.036 |
| 24.28 | (10)(10)2(11) | 0.008 | −0.014 |
| 24.13 (+0.72) [a] | (30)(30)0(11)* [b] | −0.447 | 0.405 |
| 23.98 | (10)(10)2(31) | −0.195 | 0.028 |
| 23.46 | (10)(10)2(21) | −0.069 | −0.010 |
| 23.08 | (10)(10)0(11) | −0.032 | −0.008 |
| 22.64 (+0.21) [a] | (30)(30)4(31) | 0.504 | −0.132 |
| 22.08 | (30)(30)2(11) | −0.096 | 0.034 |
| 21.78 | (30)(30)2(31) | −0.238 | 0.124 |
| 21.26 | (30)(30)2(21) | −0.667 | 0.015 |
| 20.18 | (30)(30)0(11) | −0.131 | 0.013 |

[a] Adjustments in energy used in our final calculations.

[b] The state (11)* is at 17.43 MeV.

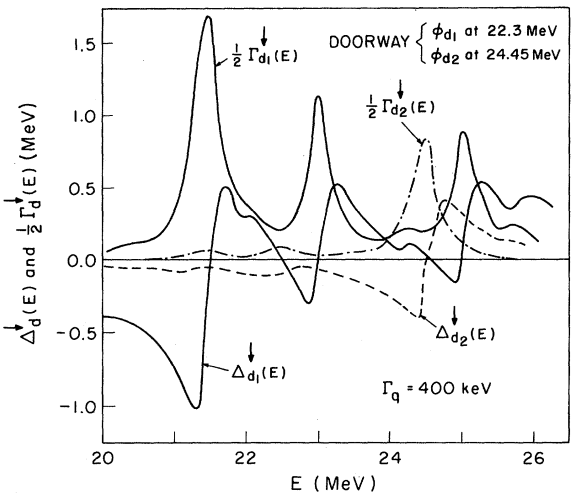


FIG. 11. The compound shifts, $\Delta_d^{\downarrow}(E)$, and widths, $\Gamma_d^{\downarrow}(E)$, of the doorways. For this calculation, the spectrum of the 3p-3h states is adjusted and the coupling matrix elements to the 22.3-MeV doorway are reduced by 15% (see Table VII). The parameter $\Gamma_q$ is taken to be 400 keV.

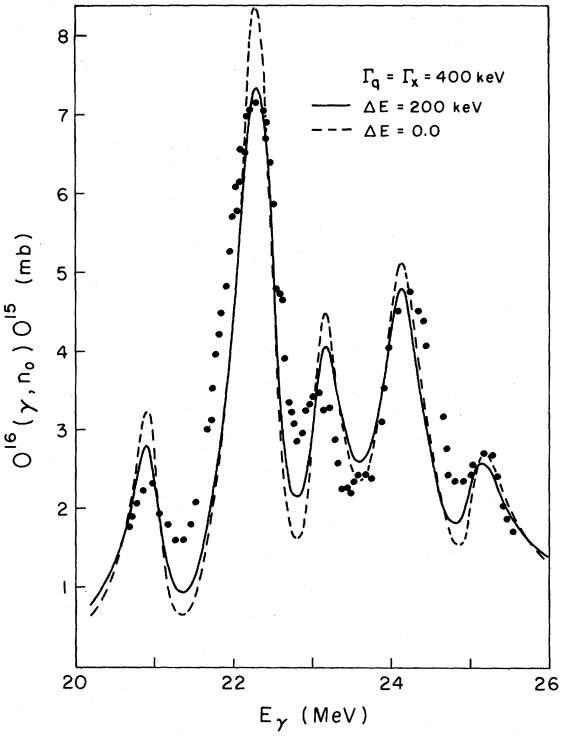


FIG. 12. The intermediate structure in $O^{16}(\gamma, n_0)O^{15}$, leading to the ground state of $O^{15}$. The experimental data are from Caldwell *et al.* (Ref. 3). The dashed line represents the intermediate-resolution cross section. The solid line is obtained from the intermediate-resolution cross section using Eq. (34) with an energy resolution $\Delta E = 200$ keV.

they remain essentially pure 3p-3h states. It is also interesting to see that the states at 22.3 and 24.2 MeV now have only 50 and 74% 1p-1h configurations, respectively. We have used the adjusted spectrum and the reduced coupling strengths in this calculation. The complete spectrum is compared with the experiment[3,4,30] in Fig. 13, where only levels with known quantum labels are shown. In Table IX we compare the dipole-strength distribution with the "strengths" obtained from various experiments. We have defined the strength for each compound state $i$, as

$$I_i = (\Gamma_\gamma^i / \sum_i \Gamma_\gamma^i) \times 100 . \quad (87)$$

(Quantity $I_i$ is not simply proportional to the integrated cross section at each resonance.) The agreement with experiment is very good. It should be noted that the experimental values are generally obtained by comparing relative integrated cross section under each resonance; this scheme is subject to large uncertainties.

From the agreement obtained in Table IX, we see that the compound states are well described in

TABLE VIII. Configuration-mixing coefficients of 3p-3h and 1p-1h states.

| Unperturbed energy (MeV) | Configuration | Eigenstate energy (MeV) 25.16 | 24.22 | 23.10 | 22.28 | 20.97 |
|---|---|---|---|---|---|---|
| 25.58 | (30)(10)2(31) | 0.121 | 0.024 | −0.037 | −0.0040 | −0.018 |
| 25.06 | (30)(10)2(21) | −0.347 | 0.030 | −0.027 | −0.0028 | −0.012 |
| 24.53 | (30)(10)3(21) | 0.016 | 0.031 | 0.031 | 0.027 | 0.011 |
| 24.85 | (30)(30)0(11)* [a] | 0.786 | −0.502 | 0.095 | 0.107 | 0.045 |
| 23.98 | (10)(10)2(31) | 0.029 | 0.040 | 0.092 | 0.068 | 0.025 |
| 22.85 | (30)(30)4(31) | −0.051 | −0.055 | 0.836 | −0.527 | −0.102 |
| 21.78 | (30)(30)2(31) | 0.025 | 0.036 | −0.071 | −0.285 | 0.113 |
| 21.26 | (30)(30)2(21) | 0.020 | −0.012 | −0.154 | −0.382 | 0.880 |
| 20.18 | (30)(30)0(11) | 0.004 | 0.000 | −0.019 | −0.037 | −0.062 |
| 22.31 | (11) | −0.126 | 0.086 | 0.499 | 0.688 | 0.442 |
| 24.45 | (11) | 0.476 | 0.856 | 0.057 | −0.035 | −0.017 |

[a] See Table VII.

our model as mixtures of one- and three-boson states. The states at 21.73 and 25.60 MeV, although containing some dipole strength, are smeared out by the intermediate energy averaging; they are not visible in the cross sections. We particularly note that the state at 21.73 MeV, with proper change in $\Gamma_q$ and $\Gamma_X$, may contribute to the lower-side asymmetry of the main peak at 22.3 MeV. This asymmetry was discussed by Greiner[11] as due to isospin-mixing of a $T=0$, 1p-1h state with the dipole state.

A careful study of Tables VII and VIII shows that the 3p-3h states containing the one-boson state ($1^-0$) as a component are not important in our calculation. This means that the elementary boson ($1^-0$) we have used may be neglected altogether; the octupole-vibration boson ($3^-,0$), on the contrary, plays a critical role in our calculation. This observation may relieve us from otherwise repudiative identification of our ($1^-0$) state at 11.32 MeV with the experimental level at 7.1 MeV, as discussed before. The ($1^-0$) state at 7.1 MeV may have much more complicated configuration; we will return to this point at our conclusion.

We now examine the structure of the *important* compound states which are responsible for the intermediate structure. The compound states at 25.16, 23.10, and 20.97 MeV all contain the two-boson states, $|(30)(30)J\rangle$. These states may be considered as two octupole vibrations ($3^-,0$) cou-

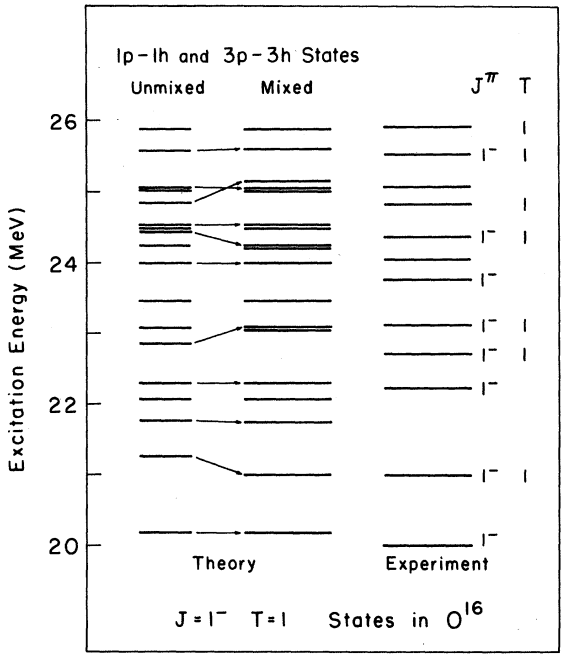


FIG. 13. Energy spectrum of $J^\pi=1^-$, $T=1$ states of $O^{16}$ in the dipole region. The unmixed spectrum is just the energy levels of the dipole 1p-1h states and the 3p-3h states as constructed in the IBA. The mixed spectrum is obtained by diagonalizing the doorway–secondary-doorway interactions. The arrow indicates the shift of the unperturbed state which constitutes the major component of the compound (mixed) state (see Table VIII).

TABLE IX. Distribution of the dipole strengths in the intermediate structure. [The strength $I$ is defined by Eq. (87).]

| Present calculation | | | Measurements | | | | | | | | | |
|---|---|---|---|---|---|---|---|---|---|---|---|---|
| | | | $(\gamma, n_0)$ [a] | | $(\gamma, p_0)$ [b] | | ($\gamma$ absorption) [c] | | | (Elliott-Flowers) [d] | |
| $E$ (MeV) | $\Gamma_\gamma$ (eV) | $I$ | $E$ (MeV) | $I$ | $E$ (MeV) | $I$ | $E$ (MeV) | $\Gamma_\gamma$ (eV) | $I$ | $E$ (MeV) | $\Gamma_\gamma$ (eV) |
| 13.48 | 115 | 0.8 | | | | | | | | 13.7 | 60 |
| | | | 17.10 | 0.5 | | | | | | | |
| 17.43 | 224 | 1.6 | 17.25 | 2.0 | 17.25 | 5.6 | 17.2 | 145 | 3 | 17.3 | 140 |
| | | | | | 18.0 | 1.5 | | | | | |
| | | | 19.0 | 4.0 | 19.0 | 4.4 | 19.0 | 250 | 5 | | |
| 19.85 | 453 | 3.3 | 19.4 | 4.0 | 19.9 | 8.6 | 19.4 | 375 | 6 | 20.4 | 20 |
| | | | 20.1 | 1.5 | | | | | | | |
| 20.97 | 1703 | 12.3 | 20.9 | 8.5 | 20.9 | 11.2 | 20.9 | 650 | 10 | | |
| 21.73 | 437 | 3.2 | 21.6 | 2.5 | 21.5 | 6.3 | | | | | |
| | | | 22.1 | 40.0 | 21.9 | 30.0 | | | | | |
| 22.28 | 4998 | 36.2 | 22.3 | | 22.4 | | 22.3 | 2500 | 33 | 22.6 | 12 000 |
| 23.10 | 2499 | 18.1 | 23.1 | 11.0 | 23.3 | 10.1 | 23.1 | 530 | 6 | | |
| | | | 24.1 | 26.0 | 23.9 | 22.0 | | | | | |
| 24.22 | 1273 | 9.3 | 24.3 | | 24.3 | | 24.3 | 1200 | 12 | 25.2 | 5800 |
| 25.16 | 1757 | 12.7 | | | | | 25.2 | 1250 | 12 | | |
| 25.60 | 183 | 1.33 | | | | | 25.8 | 1000 | 10 | | |

[a] See Firk in Ref. 3.

[b] See Denisov and Kul'chitskiĭ in Ref. 4.

[c] B. S. Dolbilkin, *Proceedings (Trudy) of the P. N. Lebedev Physics Institute*, edited by Academician D. V. Skobel'tsyn (translated by Consultants Bureau, New York, 1967), Vol. 36; See also Ref. 30.

[d] See Ref. 1.

pled very strongly through the p-p and h-h interactions. (These interactions are neglected in the harmonic approximation.) In the dynamic collective model, such two-phonon states would be coupled to the giant-dipole state *itself*. Our formulation, where this restriction does not appear, is clearly more general.

It is also possible to reformulate our theory such that each compound state (mixture of one- and three-boson states) acts as a doorway. This latter formalism would be more useful if we considered decays to channels to which both the 1p-1h states and 3p-3h states were strongly coupled. In that case the distinction between doorways and secondary doorways as discussed here, disappears in the exit channels, but still holds for the interaction $H_\gamma$.

Using our model we have explained the origin of the intermediate resonances in the dipole region of $O^{16}$. We have also calculated the $\sigma(\gamma, n)$ $\sigma(\gamma, p)$ cross sections leading the third excited states of the residual nuclei. These are shown in Figs. 14 and 15. No significant agreement can be claimed. We note that the experimental data are not well confirmed and are generally in conflict.[31] Further investigations are therefore called for.

## V. CONCLUDING REMARKS

Using a projection-operator technique, we have formulated a (unified) theory of photonuclear reactions, in which an explicit form for the $T$ matrix is obtained. This $T$ matrix is calculated to first order in the electromagnetic interaction, but is otherwise exact, see Eq. (15).

The general $T$ matrix is then written in terms of continuum states, doorways, and secondary doorways. By introducing the doorway-state hypothesis, we greatly simplify the doorway-continuum coupling, removing the rapid energy dependence due to the coupling of the $Q$ space to the continuum. In this approximation we obtain Eq. (32).

The $T$ matrix of Eq. (32) is separated into two terms: a direct term and a resonance term. The first term describes the "direct" ejection of nucleon into the continuum space, from which we have removed any single-particle resonance. The direct term is therefore a smooth function of energy. The second term, on the other hand, has a complex structure; it exhibits resonances on an energy scale smaller than that of the doorway spacings. When we use the doorway hypothesis, this strong energy dependence is completely contained in a single factor, the compound mixing $W_d^\downarrow(E)$.

We have shown that by energy averaging we may obtain a $T$ matrix which describes the intermediate structure and which is parametrized through a few parameters which are only weakly energy-dependent – see Appendix A. The energy dependence giving rise to the intermediate structure is then contained in the part of $W_d^\downarrow$, denoted as $\Delta_d^\downarrow - i\Gamma_d^\downarrow/2$, which depends only on the secondary-doorway structure. The doorways can be shown to give rise to the gross structure, by simply neglecting the factor $\Delta_d^\downarrow - i\Gamma_d^\downarrow/2$ in the $T$ matrix.

Some of the justification for the reduction of the

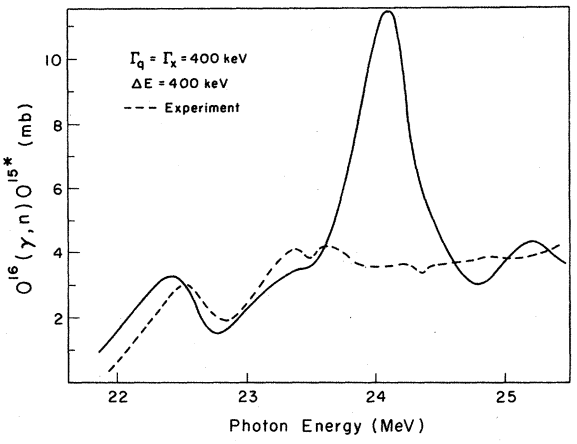


FIG. 14. The $O^{16}(\gamma, n)O^{15*}$ cross section, leading to the third excited state ($J^\pi = \frac{3}{2}^-$) of the $O^{15}$ nucleus. The experiment (the dashed line) is due to Caldwell *et al.* (Ref. 3).

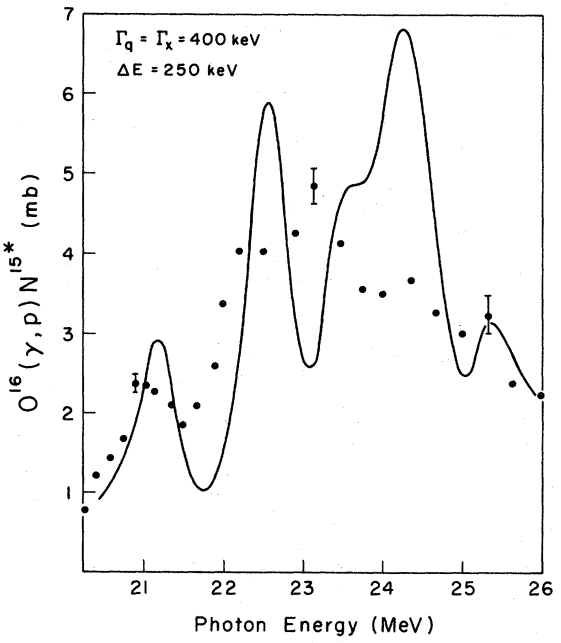


FIG. 15. The $O^{16}(\gamma, p)N^{15*}$ cross section, leading to the third excited state ($J^\pi = \frac{3}{2}^-$) of the $N^{15}$ nucleus. The experimental data is from Caldwell *et al.* (Ref. 3).

exact formal expression Eq. (15) to the form Eq. (32) is given in Sec. II. We recall that the assumption of the single-hole nature of the residual states of $N^{15}$ and $O^{15}$ allowed us to use the *same* doorways for the entrance and exit channels. If we were to consider other final channels, we would have to study the relative importance of the escape amplitudes due to the 1p-1h and 3p-3h components of the compound states formed in the reaction.

We also pointed out in Sec. II that a detailed fit to the angular distributions in the $(\gamma, n)$ and $(\gamma, p)$ reactions requires the calculation of the $E2$ and $M1$ amplitudes. If we assume that the $E2$ and $M1$ amplitudes are direct (i.e., nonresonant) in the dipole-resonance region, the variation of the *shape* of the angular distribution with energy will depend (in the doorway picture) on the interference of the more rapidly energy-dependent $E1$-doorway amplitude and the weakly energy-dependent direct amplitude.

The use of the *same* doorways for both the exit and entrance channels leads to a constant angular distribution for the various intermediate resonances associated with a single doorway, *if one neglects the direct photodisintegration amplitude*. The latter amplitude will be relatively more important at the minima of the resonant amplitude. (As mentioned previously, the interplay of these two amplitudes, one of which having rapid fluctuations in magnitude, may also account for intermediate structure in the polarization of the emitted nucleon in the case of photodisintegration leading to the one-hole states of the residual nuclei.)

Further study of the angular distributions and polarizations is clearly necessary before we can completely explore the full consequences of our model.

Our work is also dependent upon the choice of 3p-3h states as the secondary doorways. In the harmonic-oscillator shell model it is possible to obtain 2p-2h states with $J = 1^-$, $T = 1$, but only if one introduces the $2p$-$1f$ shell. (We neglect the $1s$ shell, as excitations involving that shell would be at quite high energy.) As the "$2p$-$1f$ shell" is in the continuum of a potential more realistic than the harmonic oscillator, it is very difficult to justify the inclusion of such bound oscillator states in a shell-model calculation where we pay particular attention to continuum effects. However, for relatively narrow resonances (such as the $d_{3/2}$ state considered in this work) a method has been presented which allows the incorporation of a corresponding state (a "wave packet") into the bound-state calculation. Of course, it would be of interest if one could determine experimentally the relative importance of 2p-2h and 3p-3h admixtures (with $J = 1^-$, $T = 1$) in the dipole-resonance region.

We also wish to point out that there is a great advantage in working directly with the $T$ matrix. We are able to simply adjust various parameters which we cannot calculate explicitly, to facilitate comparison with experimental data. This is an advantage over coupled-channel calculations where such modifications would be much more difficult to make.

As our results show, the shell-model description of the nucleus is quite successful, provided residual interactions are properly taken into account. Such interactions give rise to the collective nature of the dipole states. They also shift the higher configurations downward in energy and mix states with different configurations. In a straightforward application of the shell model one would have a vast number of 3p-3h states to consider as candidates for mixing with the 1p-1h dipole states. Clearly one needs to introduce some scheme that will simplify the calculations. Our success is then largely due to the use of the IBA, which successfully generates the low-lying three-boson states. Although various extensions of the IBA are possible, the approximation, as it stands, should be of interest for further applications.

In Table VIII, we have presented the results of a calculation of the compound states, i.e., mixture of doorways and secondary doorways, obtained by diagonalizing the Hamiltonian matrix. It will be interesting to see if we may obtain further evidence to support our configuration assignments for these states.

We now turn to possible extensions of our calculation. One may consider the decay of the compound states to the channels where the residual nucleus is left in low-lying positive-parity excited states.

In weak-coupling models, these positive-parity states of the residual nucleus may be described as a $1p_{1/2}$ hole coupled to the low-lying collective states of $O^{16}$. They thus have predominantly 1p-2h configurations. This is consistent with most of the results obtained by Lie, Engeland, and Dahll,[32] who also obtain admixture of 3p-4h configurations. We are particularly interested in the $\frac{5}{2}^+$ and $\frac{1}{2}^+$ excited states near 5 MeV. The $\frac{5}{2}^+$ state is described to have 82% 1p-2h configuration[32]; this state is probably a $1p_{1/2}$ hole coupled to the octupole vibration $(3^-, 0)$. We may thus deduce from their description that the 3p-3h admixture in the $(3^-, 0)$ state may be about 18%; our identification of the $(3^-, 0)$ state as pure 1p-1h is therefore approximately justified. The $\frac{1}{2}^+$ state of the residual nuclei is, however, shown to contain 65% 3p-4h

configurations.[32] If the weak-coupling description is valid, the lowest $(1^-, 0)$ state of $O^{16}$ contains about 65% 3p-3h configuration. This prediction would thus repudiate our assignment of 1p-1h nature to the $(1^-, 0)$ state of $O^{16}$. We maintain, however, that the $(1^-, 0)$ state in our calculations is so *unimportant* that our results will not be changed at all (see Sec. IV). The nature of these states, $(1^-, 0)$ in $O^{16}$ and $(\frac{1}{2}^+)$ in $O^{15}$, should be investigated further.

We note that the compound states may be coupled to the above open channels. For such consideration, we may simply relax the doorway-state hypothesis for the exit channels, or reformulate our theory to accommodate new open channels. Within our formalism, this extension immediately enables us to explicitly evalute some contributions to the parameters, $\Gamma_X$ and $\Gamma_q$, from the additional open channels placed into the $P$ space.

If the doorway-state hypothesis, in our formalism, is dropped for the exit channels, various coupling interactions in the $T$ matrix become energy-dependent on the intermediate-resonance scale. In this connection, it might also be interesting to estimate the validity of Eq. (31).

Finally we may also study the structure in photoneutron polarization measurements in the dipole region.[33] Such a calculation was performed by Buck and Hill[1] who obtain the gross structure; the data, however, show "intermediate" resonances.

On the experimental side, further investigation of the dipole region may be called for to determine the quantum numbers of the intermediate-structure resonances. Particularly related to our hypothesis is the prediction of the 3p-3h states in this region. Experiments such as $C^{13}(He^3, \gamma)O^{16}$ are of interest; the data of Puttaswamy and Kohler[34] have already shown prominent resonances at 24.1 and 25.1 MeV.

In the near future we hope to present results for the polarization cross sections and angular distribution for the photodisintegration of $O^{16}$. We hope these results will lend further support to the model discussed in this work.

*Note added in proof:* As this report was completed and ready for publication, we encountered an error in the computation associated with our multiboson states, as defined by Eq. (64). The states $|\tilde{\Phi}_q\rangle$ are not properly normalized; the normalization factor should be $[1+\delta_{12,34}]^{-1/2}$, where $\delta_{12,34}=0$ when the boson $|B_{12}\rangle$ is not identical to the boson $|B_{34}\rangle$. The corrections we have to make are as follows. In Table VI, we have to: (1) divide the diagonal matrix elements by a factor of 2, if the two bosons are identical; and (2) divide the off-diagonal elements by $\sqrt{2}$ if any of the two-boson states contains identical bosons. This would give rise to a new spectrum of 2p-2h states. In Table VII, we then: (1) recalculate the energy spectrum of the three-boson states, and (2) divide the coupling matrix elements by $\sqrt{2}$ if $|B_{12}\rangle$ is identical to $|B_{34}\rangle$ in the three-boson states. We also have to make corresponding modification in Tables VIII and IX and in Figs. 8–16. Such modifications are obvious and do not warrant a quantitative reevaluation here. Our reason may be given as follows. Keeping in mind that only *some* of the three-boson states and their coupling matrix elements in Table VII are crucial in our calculation, we may discuss the conditions under which we could preserve the features which we have obtained in Table VII, as shown. If we carry out the modifications as discussed in detail above, we find that: (1) the crucial states come out too high in energy, and that (2) their couplings to the doorways are too weak. Such discrepancies may be readily remedied by a *renormalization* of the strength of the residual interaction. For such a modification, we may increase the particle-particle and hole-hole interactions by about 45% and the particle-hole interaction in the coupling matrix elements by 20%. The modified energy spectrum is then within 1 MeV of the spectrum shown in Table VII. The coupling matrix elements are essentially identical to those used in our calculation (the values in Table VII, further reduced by 15%). With such final adjustments, we are to obtain essentially the same conclusions as reported in the text. Again the above adjustments, or the renormalization, should not be deemed as unreasonable. The approximate nature of our calculation has been discussed in the text. Aside from the neglected recoupling matrix elements, the particle-particle or hole-hole interactions may also be renormalized through core polarization, for example. It is therefore not surprising that the renormalized particle-particle and hole-hole interactions are quite different from the particle-hole interactions. A detailed discussion of such renormalization is, however, well beyond the scope of our investigation. It does not seem possible to determine the strength of the residual interaction by simply fitting the experimental low-lying states. We have chosen our strength by fitting the energies of the giant-dipole states, while Iachello has used a much stronger force to reproduce some of the low-lying, $T=0$ states of $O^{16}$ (private communication). We would like to thank Dr. F. Iachello for correspondence concerning the relative magnitudes of the particle-hole and the particle-particle hole-hole matrix elements in his calculations and ours.

ACKNOWLEDGMENT

We would like to thank Professor H. Feshbach for his interest in this work and R. L. Feinstein for pointing out a computation error in an early version of this work. One of us (W.L.W.) is indebted to Professor S. Yip for his encouragement. We are also thankful for the computer time provided by the Laboratory for Nuclear Science at Massachusetts Institute of Technology.

## APPENDIX A. ENERGY AVERAGING

In this Appendix, we shall derive Eq. (24) and show that, with some energy averaging, the quantities $\Delta_q$, $\Gamma_q$, $\Delta_X$, and $\Gamma_X$ become weakly energy-dependent. They consequently can be treated as parameters in our theory.

Dividing the $Q$ space into $X$ and $q$ spaces, we have the identity,[16]

$$\frac{Q}{E-H_{QQ}} = q\left(E-H_{qq}-H_{qX}\frac{1}{E-H_{XX}}H_{Xq}\right)^{-1}q + X\left(E-H_{XX}-H_{Xq}\frac{1}{E-H_{qq}}H_{qX}\right)^{-1}X + \text{cross terms}. \tag{A1}$$

The $q$ states and $X$ states are defined by

$$(E_q - H_{qq})|\phi_q\rangle = 0, \tag{A2}$$

and

$$(E_X - H_{XX})|\phi_X\rangle = 0, \tag{A3}$$

respectively. We now assume that the $q$ states are not coupled to one another through the $X$ states, and that $X$ states are also not so coupled through the $q$ states. Dropping the cross terms in Eq. (A1), the compound mixing, $W_d^{\downarrow}(E)$, can then be written as

$$W_d^{\downarrow}(E) = \sum_q \frac{\langle\phi_d|H|\phi_q\rangle\langle\phi_q|H|\phi_d\rangle}{E-E_q-\Delta_q+i\Gamma_q/2} + \sum_X \frac{\langle\phi_d|H|\phi_X\rangle\langle\phi_X|H|\phi_d\rangle}{E-E_X-\tilde{\Delta}_X+i\tilde{\Gamma}_X/2}, \tag{A4}$$

where the sum over $X$ states also implies integration over the continuous spectrum of $H_{XX}$. The shifts and widths in Eq. (A4) are defined as

$$\Delta_q - i\Gamma_q/2 = \sum_X \frac{\langle\phi_q|H|\phi_X\rangle\langle\phi_X|H|\phi_q\rangle}{E-E_X}, \tag{A5}$$

and

$$\tilde{\Delta}_X - \frac{i}{2}\tilde{\Gamma}_X = \sum_q \frac{\langle\phi_X|H|\phi_q\rangle\langle\phi_q|H|\phi_X\rangle}{E-E_q}. \tag{A6}$$

Finally we see that $\Delta_X - i\Gamma_X/2$, of Eq. (24), is given by

$$\Delta_X - \frac{i}{2}\Gamma_X = \sum_X \frac{\langle\phi_d|H|\phi_X\rangle\langle\phi_X|H|\phi_d\rangle}{E-E_X-\tilde{\Delta}_X+i\tilde{\Gamma}_X/2}. \tag{A7}$$

From Eqs. (A5) and (A7), we find that the quantities $\Delta_q$, $\Gamma_q$, $\Delta_X$, and $\Gamma_X$ vary rapidly in a region of energy of the order of the level spacing of the discrete spectra of $H_{qq}$ and $H_{XX}$. The rapid energy dependence of these quantities would give rise to "fine structure" in the $T$ matrix. In order to obtain a $T$ matrix which varies significantly only over the intermediate resonances, we have to introduce some energy averaging to eliminate the fine structure. Since the compound mixing, in the doorway approximation, is the only factor in the $T$ matrix [see Eq. (32)] which has strong energy dependence, we only have to average $W_d^{\downarrow}$ over some energy interval $\delta E$.

We may write the *averaged* $W_d^{\downarrow}$ and *averaged parameters* ($\Delta_q$, $\Gamma_q$, $\Delta_X$, $\Gamma_X$) as follows (using the same notations for these quantities as before),

$$W_d^{\downarrow} \equiv W_d^{\downarrow}(E+i\,\delta E/2) = \sum_q \frac{\langle\phi_d|H|\phi_q\rangle\langle\phi_q|H|\phi_d\rangle}{E-E_q-\Delta_q+i(\Gamma_q/2+\delta E/2)} + \Delta_X - i\frac{\Gamma_X}{2}, \tag{A8}$$

where [see Eq. (A5)]

$$\Delta_q - i\frac{\Gamma_q}{2} = \sum_X \frac{\langle\phi_q|H|\phi_X\rangle\langle\phi_X|H|\phi_q\rangle}{E-E_q+i\delta E/2}. \tag{A9}$$

The coupling of the doorways to the $X$ states is now parametrized by

$$\Delta_X - i\frac{\Gamma_X}{2} = \sum_X \frac{\langle\phi_d|H|\phi_X\rangle\langle\phi_X|H|\phi_d\rangle}{E-E_X-\sum_q \frac{|\langle\phi_q|H|\phi_X\rangle|^2}{E-E_q+i\delta E/2}+i\delta E/2}. \tag{A10}$$

From Eqs. (A9) and (A10), we have shown that, after an appropriate choice of $\delta E$, the quantities, $\Delta_q - i\Gamma_q/2$ and $\Delta_X - i\Gamma_X/2$, are smooth functions of energy. They can therefore be treated as (constant) parameters in our theory. The factor $\delta E/2$ appearing in the denominator in Eq. (A8) is dropped in Eq. (24) for simplicity.

## APPENDIX B. COUPLING TERMS

Here we shall present some of the angular momentum algebra necessary to obtain the recoupling terms in the doorway–secondary-doorway interactions. The analytic expressions for these terms are given in Table II. As illustration, we shall derive two typical terms, $R(1)$ and $R(3)$, in detail.

We denote the reference term by

$$L^{56}_{12,34} \equiv \langle j_1' j_2'^{-1} J | V | (j_1 j_2^{-1}) J_{12} (j_3 j_4^{-1}) J_{34} J_0, (\tilde{j}_5 \tilde{j}_6^{-1}) J_{56} J \rangle , \tag{B1}$$

where we have suppressed isospin variables. The tildes indicate that the right-hand side is a *single* interaction term, in which the pair ($j_5$ and $j_6^{-1}$) moves freely to the final ph state $|(j_1' j_2'^{-1}) JT\rangle$ as shown in Fig. 2.

In the above notation, the recoupling term $R(1)$, which is shown in Fig. 3, may be written as

$$R(1) \equiv \langle (j_1' j_2'^{-1}) J | V | (j_1 \tilde{j}_2^{-1}) J_{12} (\tilde{j}_3 j_4^{-1}) J_{34} J_0, (j_5 j_6^{-1}) J_{56} J \rangle . \tag{B2}$$

Keeping the form of the reference term in mind, we may try to couple the pair ($j_3$ and $j_2^{-1}$) together and relate Eq. (B2) to the following quantity:

$$L^{32}_{14,56} \equiv \langle j_1' j_2'^{-1} J | V | (j_1 j_4^{-1}) J_s (j_5 j_6^{-1}) J_{56} J_t, (\tilde{j}_3 \tilde{j}_2^{-1}) J_s' J \rangle , \tag{B3}$$

where $J_s$, $J_s'$, and $J_t$ are to be defined below. It is clear that Eqs. (B2) and (B3) are related by unitary transformations. The order of such transformations is not important.

Beginning with Eq. (B2), we first interchange $j_3$ and $j_4$, obtaining a phase factor $C_{34}$,

$$C_{34} = (-)^{j_3 + j_4 + J_{34}} , \tag{B4}$$

which is due to the Clebsch-Gordan coefficient in the ph state $|(j_3 j_4^{-1}) J_{34}\rangle$. In order to bring $j_2$ and $j_3$ together, we need to recouple $j_1$, $j_2$, $j_3$, and $j_4$. By standard technique,[21] we have

$$R(1) = C_{34} \sum_{J_s, J_s'} [(j_1 j_2) J_{12} (j_4 j_3) J_{34} J_0 | (j_1 j_4) J_s (j_2 j_3) J_s' J_0] \langle (j_1' j_2'^{-1}) J | V | (j_1 j_4^{-1}) J_s (\tilde{j}_2^{-1} \tilde{j}_3) J_s' J_0, (j_5 j_6^{-1}) J_{56} J \rangle . \tag{B5}$$

The recoupling coefficient in Eq. (B5) is related to a 9-$j$ symbol by[21]

$$[(j_1 j_2) J_{12} (j_4 j_3) J_{34} J_0 | (j_1 j_4) J_s (j_2 j_3) J_s' J_0] = ([J_{12}, J_{34}][J_s, J_s'])^{1/2} \begin{Bmatrix} j_1 & j_2 & J_{12} \\ j_4 & j_3 & J_{34} \\ J_s & J_s' & J_0 \end{Bmatrix} . \tag{B6}$$

Comparing Eq. (B5) with Eq. (B3), we see that the ($j_2^{-1} j_3$) pair should be moved out of the intermediate angular momentum $J_0$. We see that

$$|(j_1 j_4^{-1}) J_s (j_2^{-1} j_3) J_s' J_0, (j_5 j_6^{-1}) J_{56} J \rangle = \sum_{J_t} [(J_s J_s') J_0 J_{56} J | (J_s J_{56}) J_t J_s' J] | (j_1 j_4^{-1}) J_s (j_5 j_6) J_{56} J_t, (j_2^{-1} j_3) J_s' J \rangle , \tag{B7}$$

where the recoupling coefficient is related to a 6-$j$ symbol by

$$[(J_s J_s') J_0 J_{56} J | (J_s J_{56}) J_t J_s' J] = (-)^{J_{56} + J_t + J_s' + J_0} ([J_t, J_0])^{1/2} \begin{Bmatrix} J_s & J_{56} & J_t \\ J & J_s' & J_0 \end{Bmatrix} . \tag{B8}$$

After interchanging $j_2$ and $j_3$, we have

$$R(1) = (-)^{j_2 + j_4 + J_{34} + 1 + J_{56} + J_0} ([J_{12}][J_{34}][J_0])^{1/2} \sum_{J_s, J_s', J_t} ([J_s][J_s'][J_t])^{1/2} (-)^{J_t} \begin{Bmatrix} J_s & J_{56} & J_t \\ J & J_s' & J_0 \end{Bmatrix} \begin{Bmatrix} j_1 & j_2 & J_{12} \\ j_4 & j_3 & J_{34} \\ J_s & J_s' & J_0 \end{Bmatrix}$$

$$\times \langle (j_1' j_2'^{-1}) J | V | (j_1 j_4^{-1}) J_s (j_5 j_6^{-1}) J_{56} J_t, (\tilde{j}_3 \tilde{j}_2^{-1}) J_s' J \rangle . \tag{B9}$$

Equation (B9) can be simplified if we recall the δ-function conditions in the reference term, Eq. (80), which require

$$J_t = 0, \quad J'_s = J, \quad J_s = J_{56}; \tag{B10}$$

otherwise $R(1)$ vanishes identically. We may rewrite Eq. (B9) as

$$R(1) = (-)^{j_2+j_4+J_{34}+1+J}([J_{12}][J_{34}][J_0])^{1/2} \begin{Bmatrix} j_1 & j_2 & J_{12} \\ j_4 & j_3 & J_{34} \\ J_{56} & J & J_0 \end{Bmatrix} L^{32}_{14,\,56}. \tag{B11}$$

This expression is listed in Table II. Here we have also used the following relation:

$$\begin{Bmatrix} J_{56} & J_{56} & 0 \\ J & J & J_0 \end{Bmatrix} = (-)^{J_{56}+J+J_0}([J_{56}, J])^{-1/2}. \tag{B12}$$

For the next example, we consider

$$R(3) \equiv \langle ((j'_1 j'^{-1}_2)J \,|\, V \,|\, (j_1 j_2^{-1})J_{12}(\tilde{j}_3 j_4^{-1})J_{34} J_0, (j_5 \tilde{j}_6^{-1})J_{56} J\rangle. \tag{B13}$$

This term can be transformed, by similar steps as described above, to the following reference form:

$$L^{36}_{12,\,54} = \langle ((j'_1, j'^{-1}_2)J \,|\, V \,|\, (j_1 j_2^{-1})J_{12}(j_5 j_4^{-1})J'_s J'_t, (\tilde{j}_3 \tilde{j}_6^{-1})J_t J\rangle, \tag{B14}$$

where $J'_s$, $J'_t$, and $J_t$ are to be defined below. We shall, however, take an alternative method, making use of the result of our first example.

We may recouple $J_{12}$, $J_{34}$, and $J_{56}$ such that

$$R(3) = \sum_{J_t} [(J_{12}J_{34})J_0 J_{56} J \,|\, J_{12}(J_{34}J_{56})J_t J] \langle ((j'_1 j'^{-1}_2)J \,|\, V \,|\, (j_1 j_2^{-1})J_{12}, (\tilde{j}_3 j_4^{-1})J_{34}(j_5 \tilde{j}_6^{-1})J_{56} J_t J\rangle. \tag{B15}$$

We may now interchange (i) $J_{12}$ and $J_t$ in $|(J_{12}J_t)J\rangle$ and (ii) $J_{34}$ and $J_{56}$ in $|(J_{34}J_{56})J_t\rangle$. This gives

$$R(3) = (-)^{J_{12}+J_{34}+J_{56}+J} \sum_{J_t} [(J_{12}J_{34})J_0 J_{56} J \,|\, J_{12}(J_{34}J_{56})J_t J] \langle ((j'_1 j'^{-1}_2)J \,|\, V \,|\, (j_5 \tilde{j}_6^{-1})J_{56}(\tilde{j}_3 j_4^{-1})J_{34} J_t, (j_1 j_2^{-1})J_{12} J\rangle. \tag{B16}$$

We note now the form of the matrix element in Eq. (B16) is identical to Eq. (B2). Making use of the results of Eq. (B9), we have

$$R(3) = (-)^{j_6+j_4+J_{34}+1+J_{12}}([J_0][J_{34}][J_{56}])^{1/2} \sum_{J_t, J_s, J'_s, J'_t} (-)^{J'_t}([J_s][J'_t][J'_s])^{1/2}[J_t] \begin{Bmatrix} j_5 & j_6 & J_{56} \\ j_4 & j_3 & J_{34} \\ J_s & J'_s & J_t \end{Bmatrix}$$
$$\times \begin{Bmatrix} J_{12} & J_{34} & J_0 \\ J_{56} & J & J_t \end{Bmatrix} \begin{Bmatrix} J_s & J_{12} & J'_t \\ J & J'_s & J_t \end{Bmatrix} \langle (j'_1 j'^{-1}_2)J \,|\, V \,|\, (j_5 j_4^{-1})J_s(j_1 j_2^{-1})J_{12} J'_t, (\tilde{j}_3 \tilde{j}_6^{-1})J'_s J\rangle. \tag{B17}$$

We may now impose the following condition:

$$J_s = J_{12}, \quad J'_t = 0, \quad J'_s = J. \tag{B18}$$

The summations in Eq. (B17) are reduced to a single sum. We have

$$R(3) = (-)^{j_4+j_6+J_{34}+1+J}([J_{34}][J_{56}][J_0])^{1/2} \sum_{J_t} [J_t] \begin{Bmatrix} J_{56} & J_{34} & J_t \\ J_{12} & J & J_0 \end{Bmatrix} \begin{Bmatrix} j_5 & j_6 & J_{56} \\ j_4 & j_3 & J_{34} \\ J_{12} & J & J_t \end{Bmatrix} L^{36}_{54,\,12}, \tag{B19}$$

where we have also made use of Eq. (B12). The sum in Eq. (B19) is given as

$$\sum_{J_t} [J_t] \begin{Bmatrix} J_{56} & J_{34} & J_t \\ J_{12} & J & J_0 \end{Bmatrix} \begin{Bmatrix} j_5 & j_6 & J_{56} \\ j_4 & j_3 & J_{34} \\ J_{12} & J & J_t \end{Bmatrix} = \begin{Bmatrix} j_5 & j_4 & J_{12} \\ J_{34} & J_0 & j_3 \end{Bmatrix} \begin{Bmatrix} j_6 & j_3 & J \\ J_0 & J_{56} & j_5 \end{Bmatrix}. \tag{B20}$$

If we interchanged, in Eq. (B17), $J_s$ and $J_{12}$ in the $(J_s J_{12})J'_t$ coupling, we would have a phase factor $C$:

$$C = (-)^{J_s+J_{12}+J'_t},$$

which is positive, by Eq. (B18). So Eq. (B19), together with Eq. (B20), is identical to the analytical expression given in Table II for $R(3)$.

†Work supported in part by U. S. Atomic Energy Commission.

*Based on a dissertation of W. L. Wang submitted to Massachusetts Institute of Technology as a partial fulfillment of the requirements for the degree of Doctor of Philosophy (May, 1971).

‡ Present address: Department of Physics, Carnegie-Mellon University, Pittsburgh, Pennsylvania 15213.

[1]G. E. Brown, L. Castillejo, and J. A. Evans, Nucl. Phys. 22, 1 (1961); J. P. Elliott and B. H. Flowers, Proc. Roy. Soc. (London) A242, 57 (1957); J. D. Perez and W. M. MacDonald, Phys. Rev. 182, 1066 (1969); J. Raynal, M. A. Melkanoff, and T. Sawada, Nucl. Phys. A101, 369 (1967); S. Fujii, *ibid.* A132, 385 (1969); B. Buck and A. D. Hill, *ibid.* A95, 271 (1967); A. M. Saruis and M. Marangoni, *ibid.* A132, 433 (1969).

[2]Additional structure has been produced in eigenchannel calculation of H. G. Wahsweiler, W. Greiner, and M. Danos, Phys. Rev. 170, 893 (1968). This feature has been criticized as being spurious. See Saruis and Marangoni in Ref. 1 and C. Mahaux and H. A. Weidenmüller, Phys. Rev. 170, 847 (1968).

[3]F. W. K. Firk, Nucl. Phys. 52, 437 (1964); J. T. Caldwell, R. L. Bramblett, B. L. Berman, R. R. Harvey and S. C. Fultz, Phys. Rev. Letters 15, 976 (1965); T. A. Khan, J. S. Hewitt, and K. G. McNeill, Can. J. Phys. 47, 1037 (1969); J. W. Jury, J. S. Hewitt, and K. G. McNeill, *ibid.* 48, 1635 (1970).

[4]N. W. Tanner, G. C. Thomas, and E. D. Earle, Nucl. Phys. 52, 45 (1964); V. P. Denisov and L. A. Kul'chitskiĭ, Yadern. Fiz. 2, 70 (1965) [transl.: Soviet J. Nucl. Phys. 2, 48 (1966)]; J. E. E. Baglin and M. N. Thompson, Nucl. Phys. A138, 73 (1969); R. J. J. Stewart, Australian J. Phys. 21, 107 (1968); P. M. Tutakin, Yadern. Fiz. 8, 661 (1968) [transl.: Soviet J. Nucl. Phys. 8, 383 (1969)].

[5]B. S. Ishkhanov, I. M. Kapitonov, E. V. Lazutin, I. M. Piskarev, V. S. Sopov, and V. G. Shevchenko, Yadern. Fiz. 12, 892 (1970) [transl.: Soviet J. Nucl. Phys. 12, 484 (1971)].

[6]M. V. Mihailovic and M. Rosina, Nucl. Phys. 40, 252 (1963); S. Fujii, *ibid.* 67, 592 (1965).

[7]V. V. Balashov and N. M. Kabachnik, Phys. Letters 25B, 316 (1967); V. Gillet, M. A. Melkanoff, and J. Raynal, Nucl. Phys. A97, 631 (1967).

[8]N. P. Yudin, Izv. Akad. Nauk SSSR Ser. Fiz. 26, 1222 (1962); [transl.: Bull. Acad. Sci. USSR, Phys. Ser. 26, 1234 (1962)]; J. B. Seaborn, Phys. Rev. 179, 958 (1969); G. D. Dracoulis, M. S. thesis, University of Melbourne, 1966 (unpublished).

[9]See, for example, G. E. Brown and A. M. Green, Nucl. Phys. 75, 401 (1966).

[10]V. V. Verbinski and J. C. Courtney, Nucl. Phys. 73, 398 (1965); W. R. Dodge and W. C. Barber, Phys. Rev. 127, 1746 (1962); E. D. Earle and N. W. Tanner, Nucl. Phys. A95, 241 (1967).

[11]We shall not attempt to describe the states which may show up in the cross sections due to other mechanisms, e.g., isospin mixing and states of other multipolarities. For isospin mixing, see C. Mahaux and A. M. Saruis, Nucl. Phys. A138, 481 (1969); and W. Greiner, *ibid.* 49, 522 (1963).

[12]H. Feshbach, Ann. Phys. (N.Y.) 5, 357 (1958); 19, 287 (1962).

[13]F. Iachello, Ph.D. thesis, Massachusetts Institute of Technology, 1969 (unpublished).

[14]C. M. Shakin, Ann. Phys. (N.Y.) 22, 54 (1963); L. Estrada and H. Feshbach, *ibid.* 23, 123 (1963); W. M. MacDonald, Nucl. Phys. 56, 647 (1964).

[15]J. D. Perez and W. M. MacDonald, Phys. Rev. 182, 1066 (1969).

[16]H. Feshbach, A. K. Kerman, and R. H. Lemmer, Ann. Phys. (N.Y.) 41, 230 (1967); F. Iachello, *ibid.* 52, 16 (1969).

[17]J. Hüfner and C. M. Shakin, Ann. Phys. (N.Y.) 52, 486 (1969).

[18]For discussions in this section, one is referred to N. Auerbach, J. Hüfner, A. K. Kerman, and C. M. Shakin, Rev. Mod. Phys. 44, 48 (1972). Our assumption, $\langle \Psi_Q | H_{QP} | P\psi^{(-)} \rangle = 0$, allows us to neglect the distinction between $H_{PP}$ and $\mathcal{K}_{PP}$ in the continuum.

[19]W. L. Wang and C. M. Shakin, Phys. Letters 32B, 421 (1970).

[20]R. H. Lemmer and C. M. Shakin, Ann. Phys. (N.Y.) 27, 13 (1964).

[21]A. R. Edmonds, *Angular Momentum in Quantum Mechanics* (Princeton U. P., Princeton, N. J., 1957).

[22]J. M. Eisenberg and W. Greiner, *Excitation Mechanisms of the Nucleus* (North-Holland, Amsterdam, 1970).

[23]J. da Providência and C. M. Shakin, Ann. Phys. (N.Y.) 30, 95 (1964).

[24]W. L. Wang, Massachusetts Institute of Technology, Ph.D. thesis, 1971 (unpublished). Some errors found in this reference have been corrected in this paper. The errors also appear in C. M. Shakin and W. L. Wang, Phys. Rev. Letters 26, 902 (1971).

[25]See, for example, S. Lie and T. Engeland, Nucl. Phys. A169, 617 (1971).

[26]V. Gillet and N. Vinh-Mau, Nucl. Phys. 54, 321 (1964).

[27]The dipole-strength distribution we obtain is also quite close to that of the finite-range calculation with the Soper mixture as obtained by Brown, Castillejo, and Evans in Ref. 1.

[28]See Caldwell *et al.*, in Ref. 3.

[29]There are discrepancies in the absolute magnitudes of the measured cross sections; we, however, consider our result also in excellent agreement with other experiments in Ref. 3. Different absolute magnitudes of the cross sections may be reproduced by varying the quantities $\Gamma_X$ and $\Gamma_q$, or by "fine tuning" of the spectrum of the secondary doorways and their coupling strengths. In this work, we are only concerned with the intermediate-resonance *structure* of the cross sections.

[30]F. Ajzenberg-Selove, Nucl. Phys. A166, 1 (1971).

[31]P. F. Yergin, R. H. Augustson, N. N. Kaushal, H. A. Medicus, W. R. Moyer, and E. J. Winhold, Phys. Rev. Letters 12, 733 (1964); V. P. Denisov and L. A. Kul'chitskiĭ, Yadern. Fiz. 2, 70 (1965) [transl.: Soviet J. Nucl. Phys. 2, 48 (1966)]; R. C. Morrison, J. R. Stewart, and J. S. O'Connell, Phys. Rev. Letters 15, 367 (1965); J. T. Caldwell, Ph.D. thesis, University of California, 1967 (unpublished); Lawrence Radiation Laboratory Report No. UCRL-50287 (unpublished); K. M. Murray and J. C. Ritter, Phys. Rev. 182, 1097 (1969); H. Ullrich and H. Krauth, Nucl. Phys. A123, 641 (1969); R. O. Owens and J. E. E. Baglin, Phys. Rev. Letters 17, 1268 (1966).

[32]S. Lie, T. Engeland, and G. Dahll, Nucl. Phys. A156,

449 (1970).
[33]G. W. Cole, Jr., F. W. K. Firk, and T. W. Phillips, Phys. Letters 30B, 91 (1969); F. A. Hanser, Ph.D. thesis, Massachusetts Institute of Technology, 1967 (unpublished).
[34]N. G. Puttaswamy and D. Kohler, Phys. Letters 20, 288 (1966).

PHYSICAL REVIEW C VOLUME 5, NUMBER 6 JUNE 1972

# Two-Body Photodisintegration of $He^3$ Between 40 and 150 MeV*

Nancy M. O'Fallon,† Louis J. Koester, Jr., and James H. Smith
*University of Illinois at Urbana-Champaign, Urbana, Illinois 61801*
(Received 24 January 1972)

In an experiment with semiconductor and scintillation counter telescopes we have measured the photodisintegration cross section of $He^3$ at photon energies from 40 to 150 MeV and proton laboratory angles of 30, 60, 90, 120, and 135°.

## I. INTRODUCTION

This paper describes an experimental measurement of the photodisintegration of $He^3$ into a proton-deuteron final state for photon energies between 40 and 150 MeV. In the region from threshold to about 40 MeV, the two-body photodisintegration of $He^3$ has been moderately well studied, as has the inverse reaction.[1-11] The general features are clear. The cross section rises rapidly from threshold to a peak of 1.0 mb at an energy of 11 MeV. It then tails off to about 0.2 mb at 40 MeV.

The angular distribution is best known from the inverse reaction.[10] Here again the features are clear. The angular distribution at 15 MeV is a $\sin^2\theta$ distribution pushed toward forward proton angles near 75° in the center-of-mass system. There is essentially no isotropic component (<1%).

Theories based on fairly simple ground-state wave functions that also fit electron scattering data are capable of describing the magnitude and energy dependence of the photodisintegration. The forward peaking in this low-energy region can be understood in terms of simple retardation effects caused by the size of the nuclear wave function.[12, 13]

At energies above 40 MeV, data are rather sparse. Fetisov, Gorbunov, and Varfolomeev[6] have measured the total cross section and angular distributions, but with very limited statistical accuracy. Picozza *et al.*[14] have measured 90° differential cross sections between 180 and 500 MeV. Didelez *et al.*[15] have measured the inverse reaction for the equivalent of 109-MeV photons and have a well-determined angular distribution.

This experiment was undertaken to investigate the energy and angular dependence of $He^3$ photodisintegration from the region where it is well measured and moderately well understood in terms of photon interactions with nucleons described by a simple wave function up to meson threshold where other mechanisms for the interaction should become important.[16] An additional feature of interest is that detailed balance can be tested at 109 MeV where meson effects are not completely negligible.

## II. EXPERIMENTAL APPARATUS AND PROCEDURE

### A. Experimental Method and Arrangement

The experimental arrangement is shown in Fig. 1. The $He^3(\gamma, p)H^2$ reactions were produced by a 250-MeV bremsstrahlung beam incident on a low-temperature $He^3$-gas target. Deuterons were counted in a counter telescope consisting of three transmission-type silicon semiconductor detectors followed by a plastic scintillator. Protons were detected in time coincidence by means of a telescope of four plastic scintillators. The photon beam was horizontal. The axes of the two detector telescopes were also horizontal and could be rotated independently about the target.

The solid angle was determined by the semiconductor detectors of the deuteron telescope. The plastic scintillators of the proton telescope were large enough to intercept all protons correlated with deuterons in the deuteron telescope throughout the entire energy interval. At each angular setting, therefore, cross-section measurements for all energies were carried out at the same time.

The energies of the deuterons and protons are determined by a combination of range and pulse